Rheological Properties and Immobilization Behavior of Water-Based Polymer Coatings on Paper Using an Immobilization Cell

Aqsa Hayat

DIVISION OF PACKAGING LOGISTICS | DEPARTMENT OF DESIGN SCIENCES
FACULTY OF ENGINEERING LTH | LUND UNIVERSITY
2026

MASTER THESIS

This master's thesis has been done within the Erasmus Mundus Joint master degree FIPDes, Food Innovation and Product Design.

Funded by the European Union. Views and opinions expressed are however those of the author(s) only and do not necessarily reflect those of the European Union or the European Education and Culture Executive Agency (EACEA). Neither the European Union nor EACEA can be held responsible for them.

Rheological Properties and Immobilization behavior of Water-Based Polymer Coatings on Paper Using an Immobilization cell

A Lab-Scale Experimental Study

Aqsa Hayat

LUND
UNIVERSITY

Rheological Properties and Immobilization Behavior of Water-Based Polymer Coatings on Paper Using an Immobilization cell

A Lab-Scale Experimental Study

Published by
Department of Design Sciences
Faculty of Engineering LTH, Lund University
P.O. Box 118, SE-221 00 Lund, Sweden

Subject: Food Packaging Design (MTTM01)
Division: Packaging Logistics
Supervisor: Cedric Dicko, Lund University
Industrial supervisor: Anna Svensson, Tetra Pak Packaging Solutions AB
Examiner: Fredrik Nilsson, Lund University

Abstract

The growing demand for sustainable packaging has driven the transition from fossil-based materials to renewable alternatives, such as paper-based packaging combined with water-based coatings and adhesive. In such systems, coating performance is strongly governed by the transition from a liquid to a solid-state during application. Understanding this immobilization process is therefore essential for controlling coating quality, adhesion, and processability. This study investigates the immobilization behavior and rheological evolution of water-based polymer coatings, including polyvinyl alcohol (PVOH), starch and silk protein, using an Immobilization Cell (IMC) equipped to a modular compact rheometer. Oscillatory measurements enable simultaneous monitoring of complex viscosity and gap evolution during controlled dewatering, providing insight into concentration-driven network formation. The results reveal distinct immobilization behaviors for each polymer system. Starch exhibits the earliest and fastest transition. Silk protein shows intermediate behavior, with a more gradual development of structure. In contrast, PVOH displays the slowest response, with delayed and progressive immobilization. Additional measurements using dynamic light scattering (DLS) and bulk rheology test confirmed the stability of all polymer solutions, indicating that the observed changes are primarily governed by the dewatering process. Performance tests, including cobb and adhesion (tack) tests, were conducted to evaluate coating performance. Overall, the study highlights how different polymers respond during dewatering and immobilization. It also demonstrates that IMC is a valuable tool for understanding and optimizing water-based coatings, particularly for sustainable packaging applications.

Keywords: Immobilization Cell (IMC), Dewatering, Rheology, Water-based coatings, Polymer networks

Acknowledgment

بِسْمِ اللهِ الرَّحْمٰنِ الرَّحِيْم

First and foremost, I express my deepest gratitude to Allah, whose blessings, guidance, and support made this journey possible. It is through his mercy that I have been able to reach this stage of my academic life.

I would like to sincerely thank my parents and family for their unwavering support, endless encouragement, and constant belief in me throughout this journey. Their love and sacrifices have always been my greatest strength.

I am truly grateful to my Industrial supervisors, Anna Svensson and Parastoo Salavati, for their expert guidance, support, and valuable input throughout this work. I would also like to thank Tetra Pak Packaging Solutions AB for the opportunity to work in material science and gain insight into industrial research and innovation. My sincere thanks to my academic supervisor, Cedric Dicko, for providing insightful ideas, guidance, and valuable feedback. I also thank my examiner, Fredrik Nilsson, for his valuable feedback and support.

I am thankful to Lars Palm and Yulia Vakulenko for their continuous guidance and support throughout the program at Lund University. I also acknowledge the FIPDes program and the European Union for providing this unique opportunity and valuable international exposure. I am especially grateful to the FIPDes seniors for their guidance and support, and to the academics I met in Paris, Dublin, and Lund for their inspiration and contribution to my learning.

Finally, I would like to thank all my friends for their encouragement, support, and for bringing positivity and laughter during stressful times. Their presence made this journey much more enjoyable and memorable.

Lund, June 2026

Aqsa Hayat

Table of Contents

List of Figures

List of Tables

List of Acronyms and Abbreviations

CMC	Carboxymethyl cellulose
DH	Degree of hydrolysis
DMA	Dynamic mechanical analyzer
DMSO	Dimethyl sulfoxide
DP	Degree of polymerization
IMC	Immobilization cell
PVOH	Polyvinyl Alcohol
PVAc	Polyvinyl Acetate
PVA	Polyvinyl Alcohol
RVA	Rapid Visco analyzer

1 Introduction

This section introduces the background and motivation of the study, and outlines its key objectives, scope, and limitations.

1.1 Background and Motivation

Packaging plays a key role in ensuring food safety, quality, and shelf-life stability. In aseptic packaging, materials must provide effective barriers against oxygen, light, and microbial contamination while maintaining mechanical integrity and interlayer adhesion. These requirements enable products such as high-temperature (UHT) milk to be stored for an extended period without refrigeration (Alamri et al., 2021).

In recent years, there has been strong industry and societal push to replace fossil-based, non-renewable materials with renewable and more sustainable alternatives (Bauer et al., 2022). As a result, paper-based packaging combined with thin functional coating has become increasingly important (Eslami and Mekonnen, 2023). In such systems, water-based polymer coatings are applied onto paper substrates to provide barriers, adhesive, or sealing functionality while maintaining sustainability advantages. While these materials offer sustainability benefits, applying water-based coatings to paper presents significant processing challenges. Paper is a porous, heterogenous substrate, and when a liquid coating is applied, water is removed by absorption into paper and evaporation. This dynamic behavior strongly affects coating uniformity, adhesion, and final performance (Bakker et al., 2022).

During the coating process, the liquid formulation is applied as a thin layer that spreads across the surface and undergoes leveling before it solidifies. Proper flow and leveling are essential to achieve a uniform coating layer with consistent thickness and surface quality. These processes, however, depend strongly on how quickly water is removed and on the evolution of the coating´s rheological properties during application (Bakker et al., 2022).

A critical stage in coating application is immobilization, defined as the point at which the coating loses its ability to flow under processing stress and begins to behave like a solid, even though water may still be present. Immobilization

determines when leveling stops, how the coating structure develops, and whether defects such as poor adhesion, or non-uniform coverage occur. From an industrial perspective, controlling immobilization is therefore necessary for achieving consistent coating quality and reliable runnability (Luo et al., 2020).

The immobilization process is governed by complex interactions among the coating´s rheological properties, water removal rate, thin-film confinement and the properties of the substrate (Luo et al., 2020). Different film-forming polymers are immobilized through different mechanisms. For example, associative polymers such as poly (vinyl alcohol) (PVOH) immobilize gradually through hydrogen-bond-driven network formation and chain entanglement (Parisi et al., 2022). In contrast, polysaccharide-based systems, such as starch, can immobilize more rapidly through structural alignment and gelation (Chen et al., 2022). Protein-based polymers, such as silk fibroin, represent another category in which immobilization is driven by aggregation and conformational transitions (Boulet-Audet et al., 2013a).

From an experimental perspective, conventional rheological measurements provide valuable information about coating flow and structure at fixed composition, however, they do not measure the time-dependent evolution of properties that occur during coating application on paper. Similarly, dewatering or drying tests can quantify water removal, but they do not provide direct information about the coating´s evolving rheological response. As a result, immobilization is often studied indirectly, and its process-relevant behavior remains difficult to characterize under realistic conditions (Luo et al., 2020).

This master's thesis is motivated by the need to experimentally investigate the rheological properties of water-based coatings and how they transition from a liquid state to a solid coating during application. To achieve this, the Immobilization Cell (IMC) is used as the primary experimental tool. The Cell is operated on a modular rheometer, enabling rheological properties to be monitored. At the same time, water is simultaneously withdrawn through a porous substrate under controlled confinement.

1.2 Purpose and Objectives

The purpose of this thesis is to experimentally investigate the rheological properties and immobilization behavior of a water-based polymer coatings, including associative polymers, polysaccharides, and protein-based systems, on different paper substrates. The vision is to understand how polymer type and substrate characteristics influence the liquid-to-solid transition during coating application and how this behavior affects coating morphology, tackiness, and other functionalities for sustainable food packaging applications.

1.3 Problems/Research questions

This study addresses the following research questions:

- How do the intrinsic polymer properties influence immobilization behavior in water-based coating systems?
- How does the substrate affect the onset and development of immobilization?
- How do experimental parameters in IMC measurements (such as gap, applied force, and oscillation conditions) influence the observed immobilization behavior
- To what extent can bulk characterization methods (rheology and DLS) and performance tests be used to interpret or support immobilization behavior observed under dynamic conditions?

1.4 Scope and Delimitations

The scope of this thesis was to investigate the immobilization behavior of water-based polymer coating systems. To ensure depth of analysis within the available timeframe, the study was limited to a selected set of polymer systems, comparing associative polymers, polysaccharides, and protein-based, namely polyvinyl alcohol (PVOH), starch, and silk protein, at a defined range of concentrations and experimental conditions.

As part of the study design, two substrate types were investigated, and the IMC measurements were performed using a specific set of rheometer parameters. In addition to IMC measurements, complementary characterization techniques were used to provide a more comprehensive understanding of the coating systems. Bulk rheology and dynamic light scattering (DLS) were performed to evaluate the solution stability. Furthermore, additional tests, such as water resistance and tack measurements, were carried out to assess the practical functionality of the coatings in terms of resistance to liquid penetration and interfacial adhesion.

1.5 Structure of the Thesis

This thesis is organized as follows:

Chapter 1 introduced the research topic, outlined the problem statement, and defined the study´s objectives and hypotheses.

Chapter 2 presents the literature review, covering fundamental concepts such as film formation, dewatering, rheological behavior, and structure development in coating systems. It also introduces relevant measurement techniques and identifies gaps in current knowledge.

Chapter 3 describes the materials and experimental methods used in this work, including preparation of polymer systems, bulk characterization (rheology and DLS), and IMC measurements. Additional tests such as instant adhesion and water resistance (Cobb test) are also outlined.

Chapter 4 presents and discusses the experimental results. The behavior of different polymer systems is analyzed using IMC and bulk measurements, followed by interpretation in terms of polymer properties, substrate effects, and experimental parameters.

Finally, Chapter 5 summarizes the study´s main conclusions and provides recommendations for future research based on the findings and identified limitations.

2 Literature Review and Theoretical Framework

2.1 Sustainable Paper-Based Packaging

Food packaging plays an important role for liquids and sensitive food products, where effective barrier properties against oxygen, moisture, light, and contaminants are essential, especially in the aseptic packaging systems (Human, 2025). Simultaneously, environmental concerns and regulatory pressure have accelerated the transition from fossil-based packaging materials to renewable, recyclable alternatives.

Paper-based packaging has gained attention for its recyclability, renewability, and relatively low carbon footprint. However, paper is inherently porous and hydrophilic, resulting in insufficient performance for many food packaging applications (Kathuria and Zhang, 2022).

Surface coatings are a widely used strategy to improve the mechanical and physical performance of paper substrates. By applying thin polymer layers to fiber-based materials, it is possible to enhance their properties including oxygen and moisture barrier, grease resistance, surface strengthening, and adhesion (Kathuria and Zhang, 2022).

The effectiveness of a coating depends not only on its chemical nature but also on its ability to form a continuous, uniform film on the paper surface. Challenges such as coating penetration into the paper structure, liquid-solid transition, uneven layer formation, and defect generation can significantly reduce packaging performance (Christophliemk et al., 2023). Understanding the mechanism governing coating formation on porous substrates is therefore essential.

2.2 Film Formation and Immobilization

Film formation from water-based coatings involves a gradual transfer from a liquid-like state to a solid-like film as water is removed. At the initial stage, the coating behaves as a low-viscosity liquid that can spread and smooth surface irregularities. As water is removed, polymer concentration increases, leading to particle packing

and a rise in viscosity, that progressively restricts flow and results in film formation (Scott Bader, 2025).

When a water-based coating is applied to paper, water is removed through simultaneous surface evaporation and substrate-controlled dewatering (Christophliemk et al., 2023b). The initial penetration into the porous paper is a capillary-force-driven process that advances in ¨solid columns of varying hydrophilicity (Yang, Liu and Gu, 2013a). The paper substrate acts as a critical reservoir during the early stages, mediating moisture transport through the coating interface. As the coating layer dries and film formation progresses, the resistance to moisture transport within the coating increases, eventually making the process diffusion-controlled (Christophliemk et al., 2023b).

Coating Immobilization is the critical rheological transition where a water-based suspension loses its ability to flow under applied stress and begins to behave like a solid. This solidification is driven by the simultaneous removal of water through surface evaporation and substrate-controlled dewatering into the porous network of paper (Luo et al., 2020). The immobilization point in a coating on a paper substrate is the point at which the coating reaches a certain solid content during dewatering, after which no further redistribution of coating materials occurs. This point is important for achieving consistent high-quality coated paper and paperboard (Scott Bader, n.d.).

The onset of immobilization depends on several factors, including polymer chemistry, solid concentration, and the strength of inter-particle interactions (Luo et al., 2020). Research on various thickening systems, such as carboxymethyl cellulose (CMC), alkali swellable emulsions, and polyvinyl alcohol (PVA), indicates that the binder´s chemical nature and its ability to absorb onto the substrate directly influence the dewatering rate and the buildup of the immobilized layer (Li et al., 2019b). In coatings applied to porous substrates like paper, this transition is fundamentally coupled to substrate-controlled dewatering, in which moisture is rapidly pulled into the paper´s porous structure via capillary forces (Yang, Liu and Gu, 2013a).

2.3 Rheological Characterization of Coating Systems

Rheology is the study of the flow and deformation of materials under applied forces, for both liquids and solids. In simple terms, rheology helps answer questions such as how easily a liquid flows, how resistant it is to deformation, and whether it behaves more like a liquid or a solid under given conditions (Rodrigues, 2025). These questions are particularly important for coating systems, which must flow during application but later develop sufficient mechanical strength to form a stable film.

When a force is applied to a material, it experiences stress, which is defined as force per unit area. The material responds to stress by undergoing deformation, meaning a change in shape or size. If the deformation continues with time under constant stress, the material is said to flow. The relationship between applied stress and the resulting deformation or flow is the central focus of rheological characterization (Horwood and Nachiappan Chockalingam, 2023).

One of the most important rheological properties of coatings is viscosity. Viscosity describes the resistance of a material to flow under a specific stress, a property commonly described in everyday terms as a coating being either ¨thick¨ or ¨thin¨. While some Newtonian fluids, such as water, maintain constant viscosity across different shear rates, most coatings are non-Newtonian, often showing a decrease in viscosity under shear. In coating applications, viscosity determines how the polymers behave during pumping, spreading, and leveling on the substrate. Because coatings are exposed to different flow conditions during processing, viscosity is often measured over a range of deformation rates rather than a single value (Procopio, n.d).

In rheological measurements, deformation can be applied in many ways (Procopio, n.d.). In steady shear rheology, a continuous deformation is imposed, and the resulting behavior is measured (Wang, Shi and Shah, 2019). This approach is useful for explaining coating flows during application processes such as blade coating or roll coating (Scott Bader, n.d.). Another important rheological approach is oscillatory rheology, which applies a small oscillatory deformation rather than continuous flow to measure viscoelastic properties (Wang, Shi and Shah, 2019). In this method, the material response is separated into two components: an elastic response, which represents energy stored and recovered during deformation, and a viscous response, which represents energy dissipated as flow. These responses are quantified using the storage modulus (G′), which reflects elastic or solid-like behavior, and the loss modulus (G″), which represents viscous or liquid-like behavior (Wang, Shi and Shah, 2019). Rheology is useful for detecting network formation and collapse within coatings (Katashima, 2021).

While steady shear and oscillatory rheology provide fundamental insights into coating behavior by measuring viscosity and viscoelastic moduli, these tests are typically performed under equilibrium conditions at fixed composition (Scott Bader, n.d.). In real coating processes on paper, however, the material composition changes continuously after application. Water is removed through penetration into the porous substrate and through evaporation (Jain and Cairncross, n.d.). As a result, coating experiences a time-dependent increase in solids concentration and viscosity, accompanied by the rapid build-up of an immobilized internal structure. These complex, transient transitions cannot be adequately captured by conventional rheological measurements, which are commonly performed on bulk samples (Luo et al., 2020).

Standard rheological characterizations are typically limited because they lack the thin-film confinement and the dynamic interaction with real substrates that are essential for accurately modeling the dewatering-driven immobilization behavior observed in industrial coating processes (Christophliemk et al., 2023c). Conventional rheology, which separates material behavior from these process conditions, therefore cannot directly describe the immobilization behavior observed during coating deposition on paper (Luo et al., 2020).

2.4 Experimental approaches to study immobilization

In the paper industry, dewatering tests have been developed to evaluate how rapidly water is removed from coating formulations when applied to porous substrates and to assess the water retention and drainage behavior of paper coating colors (Jader, 2003).While such methods explain substrate-driven water removal, they are typically performed without simultaneous rheological measurement. Consequently, they cannot directly relate dewatering behavior to changes in viscosity or to the development of structure within the coating (Luo et al., 2020).

To study dewatering kinetics independently, drying ovens, and gravimetric methods are commonly used. In these approaches, the mass of a coated sample is monitored over time to determine drying rates. Such methods are useful for quantifying overall water loss and distinguishing between fast and slow drying stages (Jain and Cairncross, n.d.). However, gravimetric techniques do not provide any direct information about the mechanical or rheological state of the coating and therefore cannot identify when the coating loses its ability to flow, which is the central point of immobilization (Jain and Cairncross, n.d.; Luo et al., 2020).

Other techniques such as optical and imaging methods, including visual inspection, microscopy, and surface appearance measurements, have also been applied to study film formation and coating defects (Gutoff and Cohen, 2006; Li et al., 2019b). These methods are useful for observing leveling behavior, surface roughness, and defect development (Christophliemk et al., 2023). Nevertheless, optical techniques primarily provide qualitative information and do not directly measure the mechanical response of the coating during water removal (Luo et al., 2020).

This limitation highlights the need for an experimental approach that extends conventional rheological measurement to include active dewatering, controlled confinement, and contact with a real paper substrate. Such an approach is required to study immobilization under conditions that more closely resemble industrial coating processes, motivating the use of the immobilization cell, which is discussed in the following section.

Figure 1. Immobilization Cell (Anton Paar, n.d.)

2.5 Immobilization Cell (IMC): Principle and Relevance

The immobilization cell (IMC) was developed to study coating immobilization under conditions closely similar to practical coating processes (Jader, 2003).

The IMC can be operated in both rotational and oscillatory modes. It incorporates a porous substrate beneath the coating layer as shown in Figure 2. During the experiment, a pump is connected to the substrate side of the cell, which actively removes water from the coating through the porous substrate. This pumping action occurs via a pressure difference, mimicking substrate-driven dewatering during paper coating and allows the coating composition to change dynamically during the measurement. As water is withdrawn, the rheometer simultaneously measures the mechanical response of the coating, including changes in complex viscosity and viscoelastic behavior (Jader, 2003).

Figure 2. Anton Paar Immobilization cell showing perforated lower plate for suction-assisted dewatering and the upper geometry.

A key advantage of the IMC is that the coating is examined as a confined film, rather than a bulk sample (Luo et al., 2020). In industrial coating operations, the coating is applied as a thin liquid layer that undergoes rapid dewatering and structural evolution under dynamic conditions. In the IMC, the coating is studied within a confined geometry that enables simultaneous dewatering and rheological measurements under controlled conditions. Although the film thickness in the IMC is larger than in industrial processes, the method can allow a controlled and reproducible way to compare immobilization behavior between different materials (Jader, 2003).

The IMC does not replace conventional rheological characterization but rather extends it into a non-equilibrium regime that can be directly relevant to coating deposition on paper substrates, even though coating thickness and shear conditions are not at scale. Bulk rheology remains essential for understanding formulation behavior at fixed composition, while the IMC enables investigation of how those properties evolve during active dewatering. This makes the IMC especially suitable for comparing the immobilization behavior of different film-forming polymers under realistic coating conditions.

2.6 Water-Based Polymer Coatings for Paper Substrates

Water-based polymer coatings are widely investigated for paper packaging applications due to their low environmental impact, processability, and compatibility, with fiber-based substrates. These coatings rely on the formation of thin, continuous polymer films to impart functional properties to the paper and reduce mass transfer through paper substrate (Bakker et al., 2022).

The performance of such coatings depends on both material properties and rheological behavior during application and immobilization (Willenbacher,

Hanciogullari and Radle, 1999). Polyvinyl alcohol (PVOH), starch, and silk protein are widely used polymer systems due to their biodegradability, film-forming behavior, and compatibility with aqueous processing. These materials were selected because they represent three fundamentally different classes of polymers commonly used or studied in coating applications.

2.6.1 Polyvinyl Alcohol (PVOH) Coating

2.6.1.1 Introduction

Polyvinyl alcohol (PVOH) is a water-based polymer widely used in coatings, adhesives, packaging films, paper treatments, and biomedical products due to its strong film-forming properties, hydrogen bonding, and mechanical stability. Its biodegradability and non-toxicity have contributed to increased interest in sustainable materials research (Parisi et al., 2022).

2.6.1.2 Chemical Structure and Industrial Synthesis

Chemically, PVOH is a linear, synthetic and semi-crystalline polymer with the repeat unit –CH_2–CH(OH)– and belongs to the family of polyhydric alcohols as shown in Figure 3 (Sharma et al., 1236). PVOH cannot be polymerized directly from vinyl alcohol because the monomer is unstable. Therefore, PVOH is industrially produced by hydrolyzing (saponifying) polyvinyl acetate (PVAc), typically using alkaline catalysts such as sodium hydroxide or sodium methylate. Two molecular characteristics primarily govern the behavior of PVOH in solution and in film: the degree of polymerization (DP), which determines chain length and viscosity, and the degree of hydrolysis (DH), which represents the percentage of acetate groups converted to hydroxyls (Sharma et al., 1236).

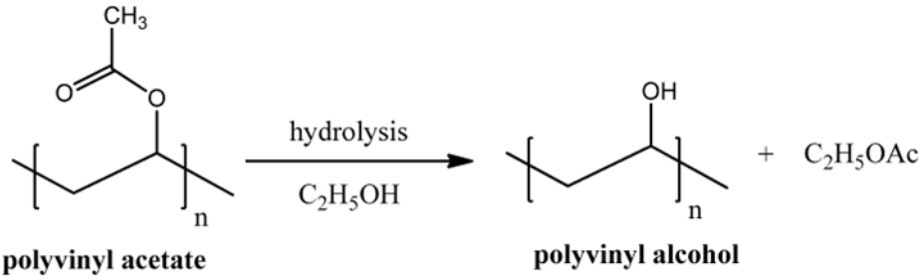

Figure 3. Chemical structure of polyvinyl alcohol derived from Vinyl acetate hydrolysis (Ehsani et al., 2022)

2.6.1.3 Degree of Hydrolysis and Polymerization

The degree of hydrolysis plays an important role in solubility, crystallinity, intermolecular interactions, and mechanical properties. (POLYVA, 2025). Fully hydrolyzed grades (98-99% DH) exhibit a high density of hydroxyl groups, which

promote strong intermolecular hydrogen bonding and more efficient chain packing, resulting in increased crystallinity. Consequently, these materials typically show higher stiffness, greater storage modulus (G′), and enhanced gel strength after drying.

In contrast, partially hydrolyzed grades (87-90%) dissolve more easily in cold water, show lower crystallinity, and form more flexible films with reduced elastic modules. This is due to residual acetate groups, which weaken chain-to-chain hydrogen bonding (Pizzo, Chiozza and Bernardini, 2024).

2.6.1.4 Concentration and Solubility Behavior

The rheological behavior of PVOH depends strongly on its concentration in aqueous solution and on temperature. At concentrations up to 10 wt%, PVOH solutions exhibit moderate viscosity, and high stability. In this concentration range, the solutions transition from a molecularly dispersed state to a complete mesh structure followed by the entanglement of molecular chains. This transition results in a strong shear-thinning (non-Newtonian) behavior, which increases sharply once the concentration exceeds a critical threshold of approximately 2-3% (Basic Physical Properties of PVOH Resin, n.d.).

At high concentrations, such as 20 wt%, the viscosity of high molecular weight PVOH increases dramatically as the mesh structure becomes denser (Basic Physical Properties of PVOH Resin, n.d.). The strong inter-and-intramolecular hydrogen bonding induced by the hydroxyl groups can lead to a temporary associative network. Research characterizes this associative polymer behavior, in which "stickers" (acetate groups) form transient hydrogen-bonded clusters or "sticky-blobs." These interactions significantly increase both the specific viscosity and the relaxation times. Such associative interactions can be effectively deactivated in strongly hydrogen-bond-accepting solvents such as DMSO, where PVOH regains the rheological scaling of a standard flexible polymer. This demonstrates that hydrogen bonding between hydroxyl groups is the dominant mechanism controlling PVOH network formation and flow behavior (Parisi et al., 2022).

2.6.1.5 PVOH during Dewatering and Drying (Relevance to IMC Theory)

PVOH is a strongly shear-thinning polymer, with viscosity decreasing rapidly under shear as polymer chains align in the flow direction. At the same time, viscosity rises sharply with polymer concentration due to chain-chain interactions. These associations lead to slow relaxation dynamics and high viscosity even at moderate shear rates (Parisi et al., 2022). These rheological attributes are directly relevant to IMC studies. During dewatering, liquid is withdrawn through a pressure difference created by a vacuum pump, causing the PVOH solutions to transition from liquid-like to solid-like behavior. As water is removed, the solids concentration increases continuously, promoting both inter- and intramolecular hydrogen bonding between the polymer chains and driving network formation (Luo et al., 2020; Basic Physical Properties of PVOH Resin, n.d.).

2.6.2 Starch and Starch-Based Coating

Starch is one of the most abundant, renewable and biodegradable polysaccharides available for industrial use, ranking second only to cellulose in natural abundance (Arruda et al., 2025). It is derived from cereals, roots, and tubers such as maize, rice, cassava, and potatoes. It has attracted significant interest due to its low cost, biodegradability, film-forming properties, and compatibility with sustainable packaging requirements (Rizwan Shoukat et al., 2025). Recent reviews emphasize starch-based films and coatings as promising candidates for replacing fossil-based plastics, particularly in paper-based food packaging and bio-composite applications. However, starch has inherent limitations, including poor water resistance and limited mechanical strength, which has led to the development of modified starch and starch-based composite coatings (Santhosh et al., 2024).

2.6.2.1 Chemical Structure, Molecular Composition, and Gelatinization

Starch is composed of two glucose-based polymers: amylose, a mostly linear α-1,4-linked molecule, and amylopectin, a highly branched α-1,4/α-1,6-linked macromolecule. The ratio between these two components strongly affects the starch functionalities (Seung, 2020). Higher amylose content typically improves film density, mechanical strength, and gas barrier properties, while amylopectin-rich starches produce more flexible but weaker films (NETZSCH, 2025).

Native starch granules exhibit a semi-crystalline structure, and when heated in excess water, they undergo gelatinization, a structural transformation characterized by granule swelling, loss of crystallinity, amylose leaching, and the formation of a viscoelastic paste. Rapid drying of starch in an amorphous state can suppress retrogradation and improve water solubility (NETZSCH, 2025).

2.6.2.2 Rheological Behavior of Starch Solutions

The rheological behavior of starch solutions is primarily governed by network formation and polymer-polymer interactions. In thermally treated or fully gelatinized starch systems, oscillatory rheology studies have shown pronounced frequency dependent behavior, including transitions from liquid-like responses ($G'' > G'$) at low frequencies to solid-like behavior ($G' > G''$) at higher frequencies, reflecting the formation of physically crosslinked networks (Santhosh et al., 2024b).

In cold-water soluble starch dispersions, structure development occurs primarily through time-dependent dewatering and concentration increase. Consequently, IMC measurements capture a kinetic immobilization process governed by concentration increases rather than by equilibrium, and frequency-dependent rheological spectra.

2.6.3 Silk Protein

In addition to polysaccharide and synthetic-based coatings such as starch and PVOH, protein-based materials have gained greater attention as sustainable alternatives for functional coatings (Saeed Paidari et al., 2024). Among these, silk protein, specifically silk fibroin derived from Bombyx mori, emerged as a promising candidate due to its excellent film forming ability, mechanical strength, biodegradability and biocompatibility (Nature.com, 2025).

2.6.3.1 Structure and Properties of Silk Protein

Silk protein, commonly referred to as silk fibroin, is a natural fibrous protein produced by silkworms and spiders and can be processed as an aqueous solution into solid fibers, films, or coatings. It is characterized by a highly ordered β-sheet crystalline structure, which contributes to its noticeable mechanical properties and stability (Wang et al., 2024). The ordered arrangement of crystalline and amorphous domains enables a combination of strength and flexibility, stemming from a multi-scale hierarchical structure that is created as a silk protein 'melt' converts to an insoluble solid (Boulet-Audet et al., 2013). This structure makes silk suitable for thin film and coating applications, including those using regenerated silk fibroin (RSF). Because RSF solutions are prepared by dialysis of aqueous protein solutions, they can be cast or coated, making silk protein relevant as a water-based film-forming system. Structural changes in silk fibroin are not only thermally driven but are strongly affected by external stimuli such as flow (shear), deformation, and solvent removal (Boulet-Audet et al., 2013b).

2.6.3.2 Rheological Behavior of Silk Protein

Reference investigated the aggregation of the kinetics of native and reconstituted silk fibroin using a combined rheology and infrared spectroscopy (Rheo-IR) approach. Their research showed that silk fibroin feedstocks behave as concentrated polymer solutions that undergo pronounced structural changes under shear stress. Shear thinning was associated with molecular alignment, while shear thickening was accompanied by aggregation and formation of β-sheet structures. It leads to a transition from liquid-like to solid-like behavior. These results clearly showed that silk protein structure development is kinetic and deformation-driven (Boulet-Audet et al., 2013b).

Silk fibroin solidifies through protein aggregation and secondary structure reorganization (Boulet-Audet et al., 2013b). The literature demonstrates that water removal and mechanical history play an important role in driving these conformational changes, enabling silk fibroin to form physical crosslinked networks during drying or processing. Consequently, silk protein represents a distinct class of film-forming polymer in which immobilization and solidification arise from aggregation and β-sheet formation rather than associative hydrogen bonding or thermal gelation (Boulet-Audet et al., 2013b).

2.7 Research Gap and Motivation of this Thesis

Previous studies show that immobilization is a central factor in paper coating, as it determines when a coating stops flowing and begins to form a stable film. Immobilization depends on several factors acting together, including polymer properties, thin-film confinement, and interaction with the paper substrate.

Conventional rheological measurements provide important information about coating flow and rheology at a fixed composition, but they do not capture how these properties change as water content is changed. Similarly, drying and dewatering tests describe water loss but do not measure the evolving rheological response of the coating. As a result, immobilization is often studied indirectly, and its full process-relevant behavior remains difficult to describe. The immobilization cell (IMC) offers a way to overcome this limitation by enabling rheological measurements during active dewatering under confined conditions and in contact with real paper substrate.

This thesis aims to improve the understanding of how polymer chemistry and substrate characteristics together influence immobilization in paper coating processes.

2.8 Theoretical Framework

This study builds its theoretical foundation on principles from polymer physics, rheology, and coating science, with a particular focus on film formation, dewatering, and structure development in water-based coating systems. Within this framework, the experimental approach is designed to test the hypothesis that immobilization behavior in such systems is governed by the combined influence of intrinsic polymer properties, substrate-controlled dewatering, and experimental conditions. Supporting this, it is further hypothesized that differences in polymer structure, substrate characteristics, and measurement parameters lead to distinct immobilization responses.

The central concept is that immobilization arises from the interaction between increasing polymer concentration and the development of intermolecular forces during solvent removal. As water is removed, polymer chains or particles are brought into closer contact, leading to a transition from a flowable system to a highly viscous or solid-like structure.

From a rheological perspective, this behavior can be understood through concentration-dependent viscosity and viscoelasticity. As polymer concentration increases, intermolecular interactions such as hydrogen bonding, entanglement, and aggregation result in a nonlinear increase in viscosity and resistance to deformation.

This provides the theoretical basis for interpreting immobilization as a competition between molecular mobility and structure formation under dynamic conditions.

The study also incorporates principles of film formation in coating systems, where the transformation from a liquid layer to a continuous film occurs through processes such as solvent removal, particle packing, deformation, and inter-diffusion of polymer chains. These mechanisms are widely used to describe structure development in water-based coatings and provide the conceptual framework for analyzing the evolution of viscosity and mechanical response observed in IMC measurements.

In addition, the role of the substrate is interpreted through capillary-driven liquid transport theory. Dewatering in porous paper substrates is governed by capillary forces, pore structure, and permeability, which control the rate of solvent removal and, consequently, the increase in polymer concentration. This provides a framework for understanding how substrate properties influence the timing and progression of immobilization without altering the underlying polymer interaction mechanisms.

From a process perspective, the study considers the effect of confinement and mechanical loading during IMC measurements. Unlike bulk measurements, IMC introduces a thin-layer geometry with an applied normal force and oscillatory deformation, enabling the investigation of structure formation under conditions that couple transport, deformation, and concentration evolution. This approach provides insight into how polymer systems respond under process-relevant constraints, even though the absolute conditions differ from those in industrial coating processes.

Overall, these rheological principles, including polymer interaction dynamics, concentration-dependent rheology, film formation mechanisms, and substrate-controlled dewatering, form the basis for the experimental design and interpretation of the results in this thesis. By applying this framework, the study aims to link intrinsic material properties with immobilization behavior observed under dynamic conditions and to provide a deeper understanding of structure–property relationships in water-based coating systems.

The experimental approach and methodology were developed to test one main hypothesis and three supporting hypotheses, which guided the selection of materials, experimental conditions, and analysis methods.

3 Materials and Methods

This Chapter presents the experimental design, and the materials and methods used to test the following hypothesis.

3.1 Experimental Design

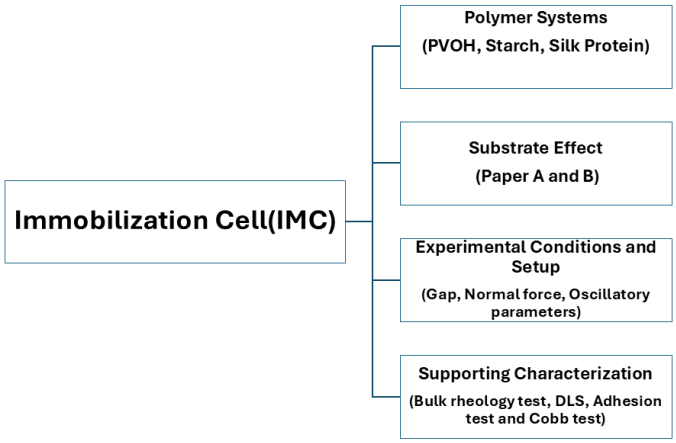

Figure 4. Schematic Diagram of Experimental Design

Figure 4 illustrates how each experimental step was developed to address a specific hypothesis. Immobilization experiments using the IMC form the core of the experimental design, as behavior of the system under dewatering conditions is the primary phenomenon investigated in this study.

3.2 Polymers

Three water-based polymer systems were selected in this study to represent different classes of coating materials such as polyvinyl alcohol (PVOH), starch, and silk protein.

3.2.1 Preparation of Polymer Solutions

PVOH is a fully water-soluble synthetic polymer that immobilizes primarily through chain association and entanglement, as concentration increases with dewatering. In this study, an industrially relevant content of 10 wt% (w/w) aqueous PVOH solution was used. A PVOH solution was prepared by adding PVOH granules to deionized water under continuous magnetic stirring and heating using a magnetic hot plate stirrer. The solution temperature was monitored with a digital thermometer inserted from the top. Stirring was maintained throughout heating to ensure homogenous dissolution of PVOH and to avoid localized concentration gradients. After complete dissolution and formation of a clear, homogenous solution, the PVOH solution was allowed to cool to room temperature under continuous stirring to maintain uniformity.

Starch was selected as a polysaccharide-based, commonly used in paper and coating formulations (Li et al., 2019b). An industrially relevant content of 40 wt% (w/w) starch solution was used, prepared by dispersing starch in deionized water under continuous stirring. Furthermore, mixing continued until visually homogenous and consistent dispersion was obtained.

After preparation, PVOH and starch solutions were allowed to degas overnight at room temperature prior to experimentation to remove entrapped air bubbles.

Silk fibroin was prepared from Bombyx mori cocoons following the protocol described by Rockwood et al. (2011). Raw silk cocoons were first cut into small pieces and boiled for 30 min in a 0.02 M sodium carbonate (Na_2CO_3) solution to remove sericin, the water-soluble protein coating surrounding fibroin. The degummed fibers were then rinsed thoroughly with ultrapure water three times for 20 min each to remove residual sericin and chemicals. The purified silk fibroin was subsequently dried overnight under ambient conditions. The dried fibroin fibers were dissolved in 9.3 M lithium bromide (LiBr) solution at a ratio of 1 g silk to 4 mL LiBr and the mixture was incubated at 60 °C for 4 h until a homogeneous solution was obtained. The resulting silk fibroin solution was transferred into dialysis cassettes and dialyzed against ultrapure water for 48 h to remove the salt. The dialysis water was changed repeatedly to ensure complete removal of LiBr. After dialysis, the solution was centrifuged twice to remove impurities and insoluble particles. The final aqueous silk fibroin solution had a concentration of approximately 7–8% (w/v).

The obtained silk fibroin solution was further concentrated to 40, 60, and 76 mg/ml, which were used for subsequent experiments.

3.3 Paper Substrates

Two paper substrates were used in the IMC experiments, referred to as Paper A and Paper B, see Table 1.

Paper A is a Kraft-type paper characterized by relatively high porosity and liquid absorption capacity. Paper B is a denser and less porous substrate exhibiting lower liquid permeability and slower water penetration. The use of these substrates with contrasting dewatering characteristics enabled direct investigation of substrate-controlled effects on dewatering and coating performance (Bing, 2025).

Table 1. Generalized properties of Paper A and Paper B used as substrates in this study

Property	Paper A	Paper B
Thickness	Thicker	Thinner
Density	Moderate	Higher
Surface roughness	Rougher surface	Smoother surface
Wettability	More hydrophobic	-
Porosity	More porous (lower air resistance)	Less porous (high air resistance)
Water absorption (Cobb value)	Higher absorption	Lower absorption

Circular paper samples were prepared using a precision cutting machine to ensure consistent geometry and reproducible contact conditions during IMC measurements. Each paper disc was cut with clean, well-defined edges to minimize edge effects. The paper was cut into circular discs with a diameter of approximately 64 mm corresponding to the bottom sieve plate diameter used in the immobilization cell, as shown in Figure 5. Prior to each experiment, a fresh paper disc was placed centrally on the IMC´s metal sieve bottom plate to ensure full contact and uniform dewatering conditions.

Figure 5. Diameter of circular paper substrate used in IMC experiments

3.4 Immobilization Cell (IMC)

3.4.1 Principle of the Immobilization Cell

Immobilization experiments were carried out using a rheology-based immobilization cell (IMC) mounted on a Modular Compact Rheometer MCR302. The IMC setup used in this study is a commercially available Anton Paar configuration.

The working principle is illustrated in Figure 6.

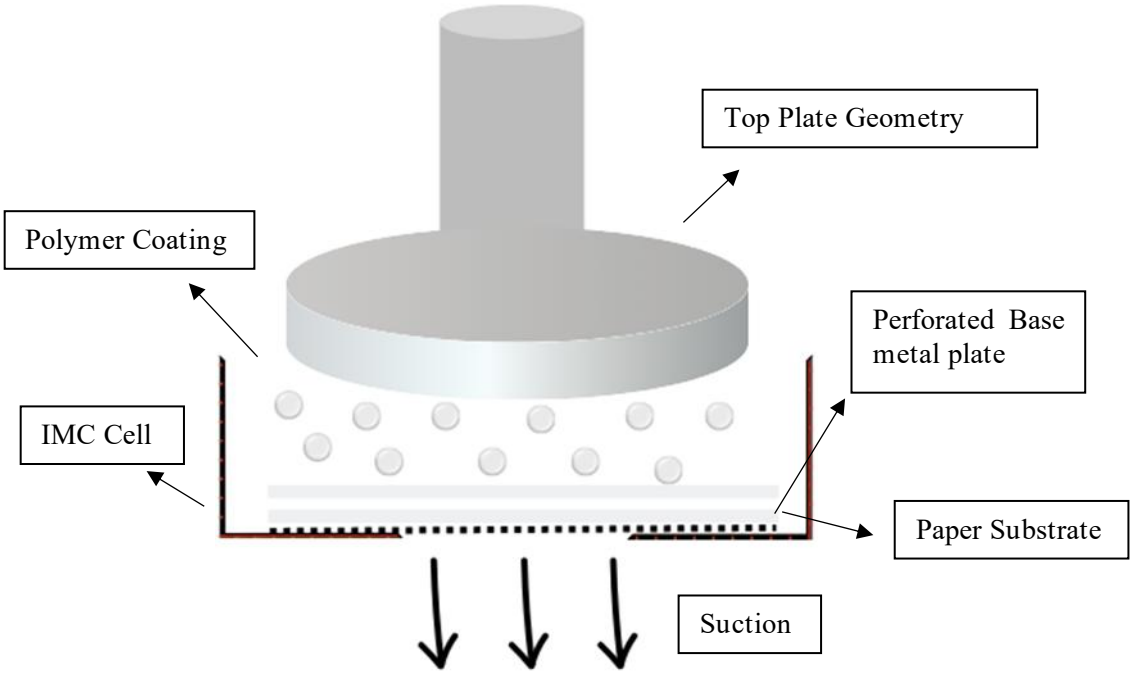

Figure 6. Schematic representation of the IMC showing the measuring top plate geometry, polymer film, paper substrate, permeable support, and suction-driven dewatering

In this configuration, a thin layer of polymer solution is confined between the upper rheometer geometry and a paper substrate placed on a permeable support. A controlled suction applied beneath the substrate induces liquid removal through the sieve plate, resulting in a progressive increase in polymer concentration within the film.

To monitor this process, oscillatory shear deformation is applied during the upper measuring geometry´s oscillatory motion, which undergoes small-amplitude oscillations to impose shear on the confined polymer film. The rheometer applies small-amplitude oscillatory strain and measures the material´s stress response.

From this response, viscoelastic properties such as complex viscosity (η^*), are determined as a function of time. Complex viscosity is calculated from the complex modulus G^*, which is composed of the storage modulus G' and the loss modulus G'', and is defined as $\eta*=G*/\omega$ where ω is the angular frequency. Simultaneously, the rheometer records the normal gap between the measuring plates. The change in gap reflects the decrease in film thickness due to liquid removal. The combined measurement of rheological properties and gap evolution enables real-time observation of the transition from fluid-like behavior to an immobilized state, characterized by a significant increase in viscosity and a reduction in gap.

3.4.2 Experimental Setup and Measurement Procedure

Prior to each experiment, the gap was first zeroed on the bottom steel sieve plate of IMC to establish a reference position. After zeroing, the measuring plate geometry was raised to a loading height of 60 mm to allow sample application. After sample loading, the geometry was lowered to the predefined gap of 0.3 mm, in accordance with the recommended operating conditions from Anton Paar.

For each experiment, a defined volume of polymer solution was applied onto the substrate using a pipette in slight excess to ensure complete coverage without overflow or incomplete spreading. The applied volume was determined by ensuring that the sample filled the measurement gap when lowering the upper geometry.

The applied volume was adjusted according to the substrate dimensions and absorption characteristics to ensure uniform coverage within a defined circular test area (diameter≈ 55 mm, see Figure 7), rather than across the entire paper sheet. For PVOH and starch systems, 2.0 ml was applied on paper A and 1.5ml on paper B. For silk protein solutions, lower volumes were used: approximately 1.0 ml applied on paper A and 0.5ml to paper B.

Figure 7. Measurement of the circular sample holder used to define coating area. The diameter of the test region is 54.8 mm, as measured using a digital caliper

Following sample loading, the geometry was lowered to the predefined initial gap of 0.3 mm. Oscillatory shear deformation (strain amplitude 0.5%, frequency 1 Hz) was applied throughout the experiment. The normal force was set to zero to ensure that the geometry followed the sample during dewatering without applying excessive compressive forces.

An initial gap of 0.3 mm indicates compaction of the wet coating and paper substrate. To obtain stable measurement conditions for immobilization, the first data points were collected without suction from the pump for 60s (corresponding to approximately 30 data points), see Figure 8. This was done to allow the sample to elevate after compression in the measurement gap. After this stabilization period, suction was applied beneath the substrate to initiate dewatering.

Measurements continued while both rheological properties and gap evolution were recorded over time. The experiment continued until immobilization was reached, as indicated by a plateau in viscosity and gap, or until no further significant changes in the measured signal were observed.

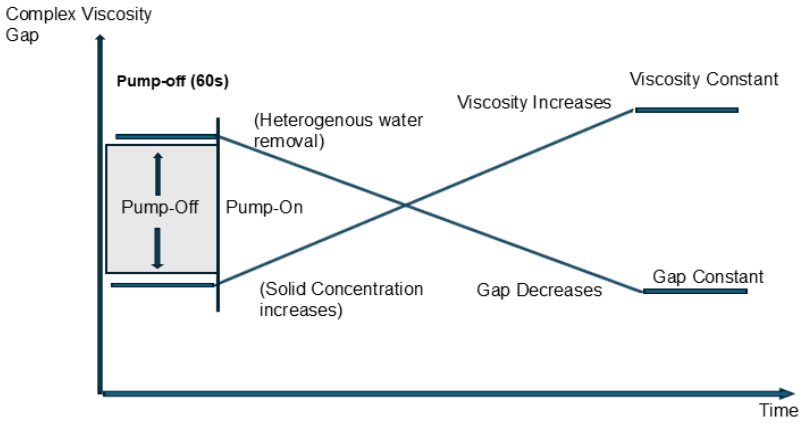

Figure 8. Schematic representation of the process followed for Immobilization Cell

3.5 Characterization and Supporting Methods

3.5.1 Dynamic Light Scattering (DLS)

Dynamic light scattering (DLS) measurements were performed to investigate the solution stability of the polymer systems and their temporal evolution. DLS probes the Brownian motion of species in solutions and enables the determination of their characteristic dynamic size. Fluctuations in scattered light intensity arise from the translational motion of polymer chains or aggregates. Analysis of the intensity autocorrelation function yields a diffusion coefficient, which can be converted into a hydrodynamic radius using the Stokes-Einstein relationship. Changes in the measured size distribution may therefore indicate aggregation, association, or loss of stability (Malik, Mays and Shah, 2021).

The purpose of performing DLS measurements in this study was to monitor whether the polymer solutions remained homogeneous and stable over time, to assess transparency and the presence of aggregation, and to understand whether time dependent changes in solution structure could influence the immobilization behavior observed in the IMC.

Measurements were conducted at multiple scattering angles, including forward, side and back scattering, to assess the robustness of the obtained size distributions for

PVOH and starch solutions at different times from Day 0 to Day 3. Sample preparation of polymer solutions is described in section 3.1.

3.5.2 Rheological Characterization (Cone-and-plate geometry)

Rheological measurements were performed using a Modular Compact Rheometer 702e equipped with cone-and-plate geometry (CP50-1), see Figure 9.

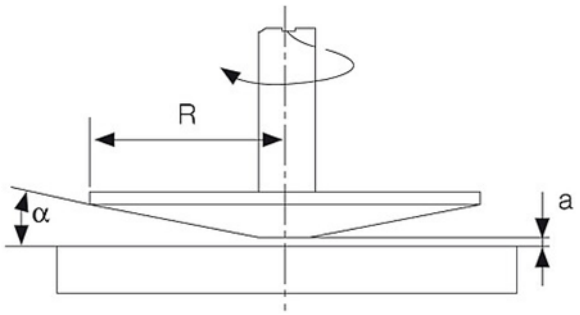

Figure 9. Cone-plate system with radius R, Cone angle α, and truncation (Anton Par, n.d.)

The sample was confined between the cone and plate, and no vacuum or solvent transport effects were present during measurement. Oscillatory shear measurements were conducted, including amplitude sweeps to identify the linear viscoelastic region and frequency sweeps to evaluate the relative contribution of elastic and viscous behavior. Measurements were performed on PVOH and starch solutions over multiple preparation days, from day 0 to day 3. Silk protein solutions were measured on day 1 and day 2 due to limitations in sample availability.

3.5.3 Coating Adhesion and Printability Assessment

Adhesion at short times frame was screened using a laboratory rod coater.

In this method, a defined amount of polymer solution was applied as a straight line onto a paper substrate. A second paper sheet was then placed on top of the coated surface. A write-wound rod was used to spread the solution uniformly between the two sheets, forming a thin film at the interface.

Adhesion behavior was evaluated by separating paper sheets at different time intervals. Immediate separation (0 min) was carried out to assess wet adhesion and coating transfer behavior. Additional separation after a short drying period (approximately 1 min) was performed to evaluate adhesion development at short

time frame. The extent of coating transfer and fiber tearing was visually assessed. Coating transfer indicates the degree of interaction between the coating and substrate, while fiber tearing reflects strong adhesion exceeding the internal strength of the paper.

The adhesion assessments were conducted for starch, PVOH, and silk protein systems.

3.5.4 Water Resistance Measurement (Cobb Test)

Water resistance was assessed using the Cobb test to quantify liquid uptake. Cobb values are used to evaluate the influence of polymer type and water absorption behavior of the coated substrates.

Coatings were applied onto the paper substrates using a laboratory MSK-AFA-I compact tape-casting coater. The polymer solution was applied as a straight line onto the substrate and spread uniformly using the applicator to obtain a controlled and reproducible coating layer with a wet coating thickness of 15 micrometers. The coated samples were subsequently dried under ambient conditions. Two layers were applied per substrate.

Figure 10. Film applicator (Rod coater), used for film coating

The Cobb test was performed following standard procedures (ISO-535) with an exposure time of 45 s (30 s+15 s). Test specimens were cut to dimensions larger than the test area and weighed prior to measurement. Each specimen was placed on a metal base, and a metal cylinder was affixed onto the surface. A defined volume of distilled water (100 ± 5 mL) was introduced into the cylinder, and the contact time was maintained for 30 s. After this period, during the following 15 s, excess water was removed, the cylinder was detached and the test specimen was placed

between blotting papers to remove surface moisture, followed by rolling with a standard metal roller to ensure consistent blotting.

The samples were then reweighed to determine the mass again. The cobb value (at 45 s = 30 s + 15 s), expressed in g/m², was calculated based on the following equation.

Equation 1. Cobb test equation

$$\text{Cobb value} = \text{Final mass per unit area} - \text{Initial mass per unit area} * 100$$

For each polymer system, three replicates were performed. Cobb tests were conducted for PVOH, starch and silk protein solutions.

3.6 Data Selection, Reproducibility, and Exclusion Criteria

Each experiment's condition was repeated to assess reproducibility. Only datasets exhibiting stable contact, controlled gap evolution, and physically meaningful rheological responses were included in the results and discussions.

Early exploratory experiments dominated by mechanical artefacts such as uneven spreading, uncontrolled gap collapse, or pump instability were excluded from analysis, see further discussion in result section 4.1.4. These experiments were important experiences to establish stable operating conditions but were not suitable for quantitative interpretation.

Representative datasets were selected to explain consistent immobilization behavior under defined conditions, in accordance with experimental practice in rheological and process-oriented studies.

4 Results and Discussions

The results show that immobilization arises from the interplay of three key factors: intrinsic polymer properties, substrate-controlled dewatering, and experimental conditions associated with the measurement setup. This framework serves as a guide for organizing and interpreting the findings presented in the following sections, where each factor is analyzed both individually and in combination.

4.1 Results

4.1.1 Polymer-Dependent Immobilization Behavior

In this section, Paper A is used as a reference substrate to investigate polymer-dependent immobilization behavior. All IMC experiments were performed using an identical measurement protocol on paper A, so that observed differences in immobilization dynamics can be attributed primarily to the polymer´s intrinsic properties. (The influence of substrate properties is addressed separately through comparison between paper A and paper B, see section 4.1.2.)

4.1.1.1 Poly (vinyl alcohol) (PVOH)

The IMC response of the PVOH coating on Paper A shows a characteristic evolution of both complex viscosity and gap, see Figure 11.

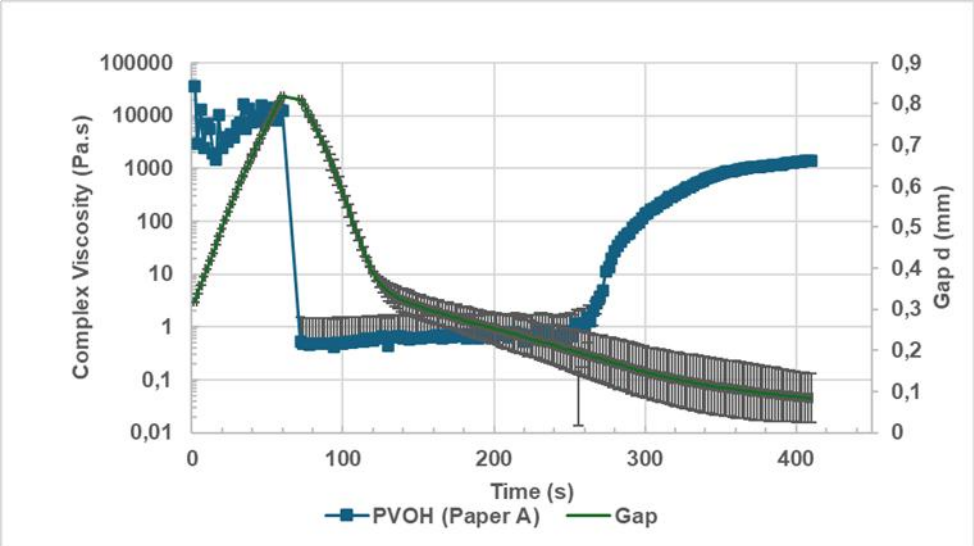

Figure 11. Complex viscosity (blue squares, left y-axis) and gap (solid line, right y-axis) during IMC measurement of PVOH coating on paper A. The complex viscosity and gap are shown as average curve based on three replicates, with error bars indicating variability between measurements.

During the initial pump-off phase (~0–60 s), the gap is set to the value of 0.3 mm and increases gradually, which can be attributed to the relaxation and slight swelling of the paper substrate upon wetting. The measured complex viscosity appears relatively high and fluctuating, which does not represent the intrinsic rheological behavior of the PVOH system. The coating layer in contact with the plate leads to unstable measurements. Upon starting of the pump suction, the gap decreases rapidly until reaching a knee point at approximately 100-120 s. This knee marks a transition from rapid water removal to a regime dominated by structural consolidation, where the fiber networks begin to resist further compression, and the removal of free water becomes limited. Beyond this point, the gap decreases more gradually toward ~0.1 mm due to progressive deswelling and densification of the fiber network under suction. The viscosity upon starting of the pump drops to low values (~1 Pa·s), indicating that the system behaves as a liquid under well-defined conditions. The continuous substrate-driven dewatering leads to a gradual increase in polymer concentration, seen as a small viscosity increase over an extended period. Then, complex viscosity rises from values below 1 Pa·s to values on the order of 10^2–10^3 Pa·s, several hundred seconds after the pump start, reflecting the non-trivial process of simultaneous absorption of the polymer into the substrate and solidification of the polymer coating.

4.1.1.2 Starch

In contrast to PVOH, the starch system exhibits a more rapid immobilization response as shown in Figure 12.

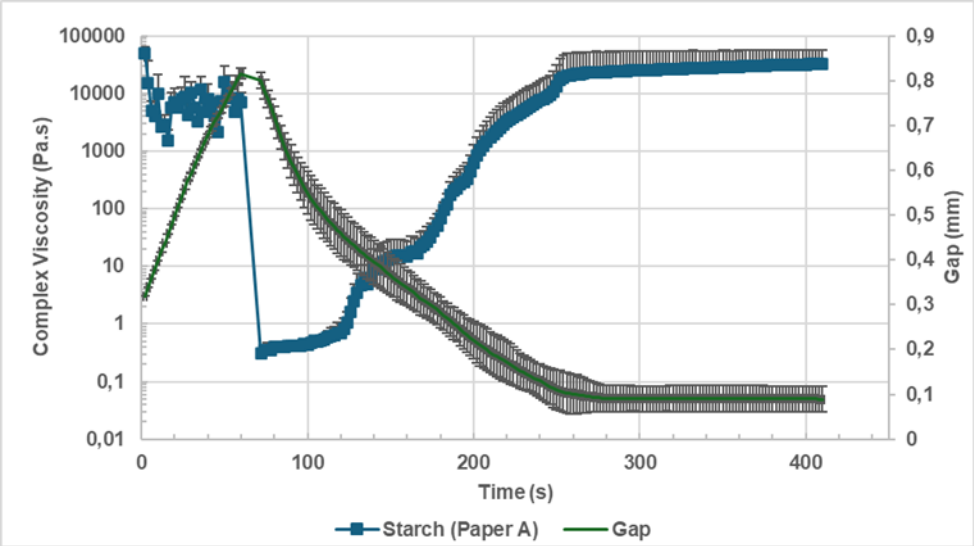

Figure 12. Complex viscosity (blue squares, left y-axis) and gap (solid line, right Y-axis) during IMC measurement of starch coating on paper A. The complex viscosity and the gap are shown as average curve based on three replicates, with error bars indicating variability between measurements.

During the pump-off phase (~0–60 s), the complex viscosity is unstable as the gap increases. Following pump activation (t ≈ 80 s), the gap decreases progressively, as the water is removed from the system and the swollen paper structure begins to compact. This fast decrease continues until about 200-250s, where a clear change in behavior (a ¨knee¨) appears at a gap of roughly 0.1-0.2 mm. After the knee, the gap only decreases slightly and gradually reaches a near-constant value, indicating that the system is close to its final film formation state. The complex viscosity increases abruptly at the onset of the pump. There is a sharp increase in viscosity to values on the order of 10^3–10^4 Pa·s, within a short time interval (~50–100 s), marking increased concentration as the starch chains begin to interact and form a hydrogen-bonded network, and the onset of immobilization (Yang, Liu and Gu, 2013). The small fluctuations and irregularities observed in the signal arise because the rheometer response is influenced by local structural variations, compression effects, and heterogenous resistance within the film, rather than purely viscous flow.

4.1.1.3 Silk Protein

IMC responses of complex viscosity and gap of three silk protein concentrations (40, 60, and 76 mg/ml) on paper A are presented together in Figure 13 and Figure 14.

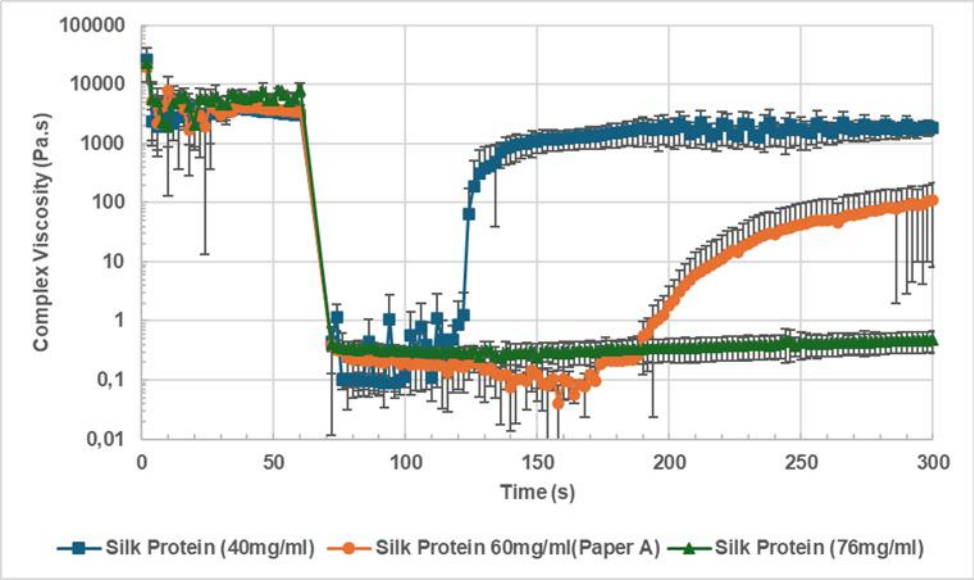

Figure 13. Complex viscosity during IMC measurement of silk protein coatings at different concentrations 40 (blue squares), 60 (orange circles) and 76 mg/ml (green triangles) on paper A. The complex viscosity is shown as average curve based on three replicates, with error bars indicating variability between measurements.

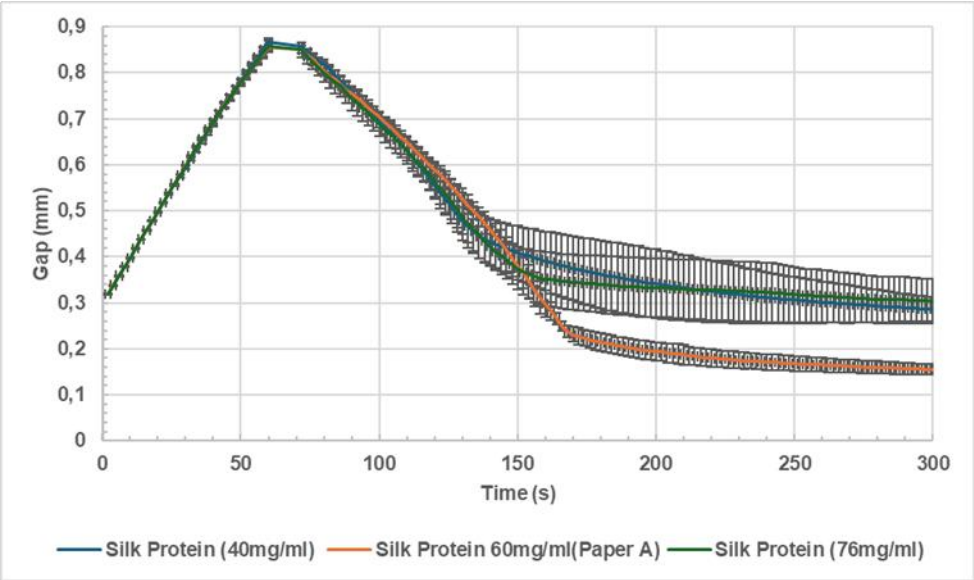

Figure 14. Gap during IMC measurements of silk protein coatings at different concentrations of 40 (blue line), 60 (orange line) and 76 mg/ml (green line) on paper A. The gap is shown as an average curve based on three replicates, with error bars indicating variability between measurements.

During the pump-off phase (0-60 s), all silk protein systems display high values of fluctuating complex viscosity similar to starch and PVOH.

After pump activation (t = 80 s), the onset and consolidation of immobilization differ markedly across silk concentrations. For the 40 mg/ml silk system, immobilization onset occurs relatively early (≈ 110–130 s), seen as a rapid increase in complex viscosity from unstable data points at approximately 0.5 Pa·s to ~10^3 Pa·s within a short time frame. This viscosity increase coincides with a pronounced decrease in gap from 0.9 mm to around 0.3 mm, see Figure 14, indicating rapid aggregation and film consolidation.

In contrast, the 60 mg/ml silk system exhibits a delayed but more gradual immobilization response. The viscosity increases from approximately 0.1Pa·s to values on the order of 10^2–10^3 Pa·s over an extended time interval (≈ 80–100 s), while the gap decreases smoothly to approximately 0.2 mm. This behavior indicates slower aggregation and consolidation compared to the 40 mg/ml system.

For the 76 mg/ml silk system, immobilization onset is further delayed and less pronounced. The viscosity increase remains limited, with low values over the whole measurement window, and the gap decreases gradually.

Overall, these results demonstrate that silk protein immobilization varies strongly with silk concentration with differences observed in onset time, viscosity evolution, and gap reduction.

Based on the stable results with balance between immobilization clarity, signal stability, and reproducibility, the 60 mg/ml silk protein was selected as a representative concentration for subsequent testing.

4.1.1.4 Comparative Analysis of Polymer-Dependent Immobilization Behavior on Paper A

Following the individual analysis of each polymer system, a direct comparison was conducted to evaluate differences in immobilization behavior on reference paper A as shown in Figure 15 and Figure 16.

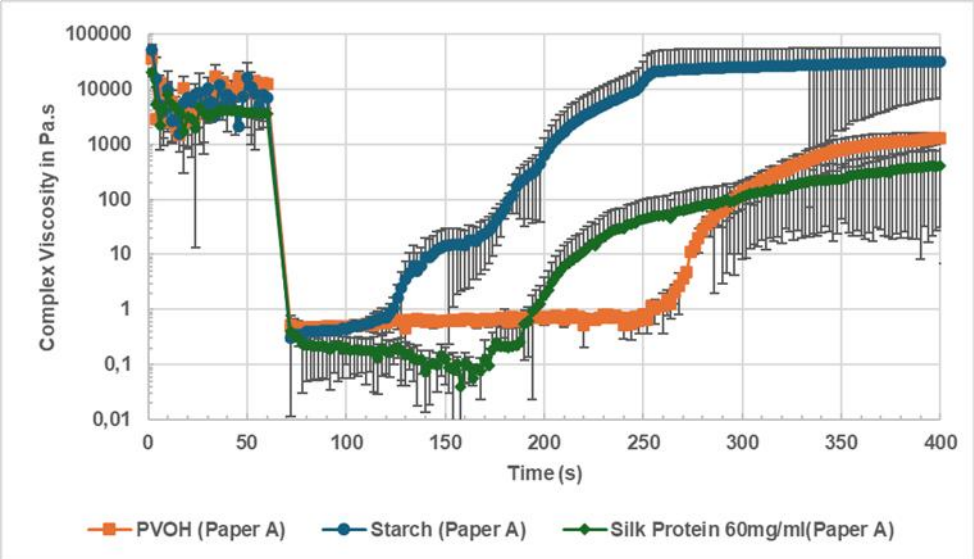

Figure 15. Comparison of complex viscosity during IMC measurements of PVOH (orange squares), starch (blue circles) and silk protein 60 mg/ml (green triangles) on Paper A. The complex viscosity is shown as an average curve based on three replicates, with error bars indicating variability between measurements.

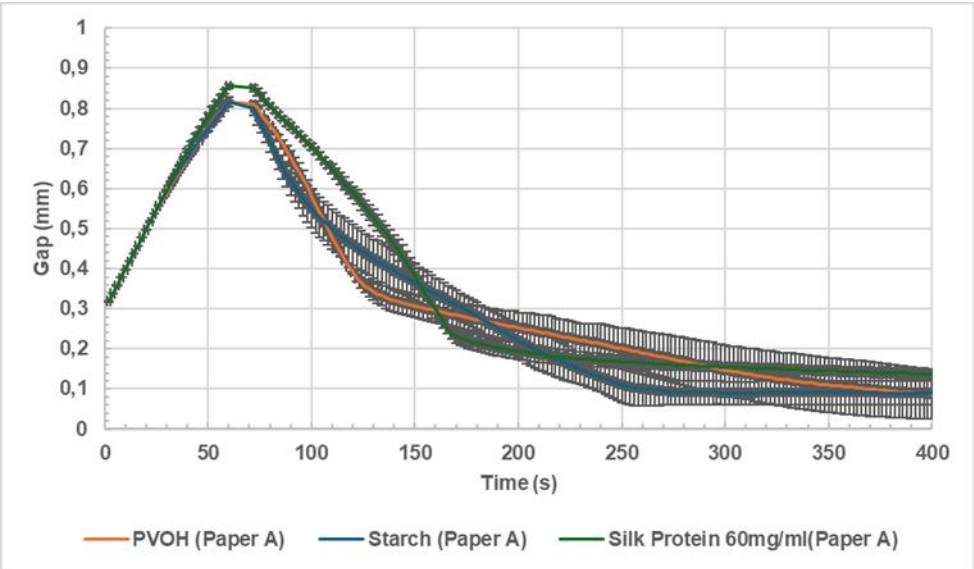

Figure 16. Comparison of gap during IMC measurements of PVOH (orange line), starch (blue line) and silk protein 60 mg/ml (green line) on paper A. The gap is shown as an average curve based on three replicates, with error bars indicating variability between measurements.

Starch exhibits the earliest onset of immobilization, with a rapid viscosity increase beginning at approximately 150-170s. This rapid increase is accompanied by a fast reduction of gap compared to the other systems, decreasing from ~0.8 mm to ~0.4 mm at approximately 110-120 s. A distinct "knee" is observed at ~0.10 mm, where the slope of the curve decreases significantly. The rapid collapse in gap coincides with the sharp increase in viscosity and reflects fast densification of the starch system.

The silk protein (60 mg/ml) shows intermediate behavior. The onset of immobilization occurs at approximately 180-200s, with a progressive rise from ~1 Pa·s to ~10^2–10^3 Pa·s. The gap decreases continuously during this period, but more gradually than in starch, from ~0.8 mm at ~60 s, to approximately 0.2 mm at 200-220 s, with a moderate knee observed at approximately 0.25-0.30 mm. This indicates a more gradual transition from structural collapse to stabilization. In contrast, PVOH exhibits the most delayed immobilization response. The onset of viscosity increase occurs at approximately 260-280 s, with a gradual rise from 1 Pa·s to a plateau in the range of ~10^2–10^3 Pa·s. The transition occurs over a longer time interval (~100–120 s) indicating slower network development and delayed transition to a solid-like structure. The gap reduction for PVOH is the most gradual extended.

Overall, the systems can be ranked by immobilization behavior as follows: Starch shows the earliest onset and most abrupt transition; silk protein exhibits immediate, moderately progressive behavior, and PVOH shows the latest onset and most gradual transition.

To facilitate comparison, key immobilization characteristics for each polymer are summarized in Table 2.

Table 2. Comparative Summary of Polymer Immobilization Behavior

Polymer	Onset of Immobilization (s)	Viscosity increase range	Duration of transition (s)	Gap reduction behavior	Overall behavior
Starch	~130–150 s	~10 to 10^4–10^5 Pa·s	~90	Rapid decrease and pronounced knee (0.10-0.15 mm).	Earliest, sharp transition
Silk Protein	~180–200 s	~1 to 10^2–10^3 Pa·s	~ 95 s	Gradual decrease with moderate	Intermediate

(60 mg/ml)				knee ~0.25–0.30 mm)	
PVOH	~260–280 s	~1 to 10^2–10^3 Pa·s	~110 s	Smooth decrease with late but distinct knee (~0.30 mm)	Latest, most gradual

4.1.2 Substrate Comparison

To evaluate the influence of substrate properties on immobilization behavior, the IMC response for identical polymer systems was compared between Paper A and Paper B under identical experimental Conditions.

4.1.2.1 Pre-Dewatering Behavior and Substrate Swelling

Differences between the substrates are already apparent during the pump-off phase. For all polymer systems, the gap initially increases due to liquid penetration into the paper and associated fiber swelling. However, the extent of this increase differs significantly.

For paper A, a pronounced increase in gap is observed, indicating substantial liquid uptake and strong swelling of the paper structure. This behavior reflects its open and permeable fiber network. In contrast, paper B shows only a limited increase in gap, consistent with restricted liquid penetration due to its dense structure and less porosity.

This early-stage behavior shows that substrate effects are not limited to dewatering but also influence the coating layer′s initial state prior to immobilization, thereby setting the conditions for subsequent film formation.

4.1.2.2 PVOH on Paper A and Paper B

Figure 17 and Figure 18 show that, for PVOH, substrate effects are significantly greater when comparing Paper A and Paper B.

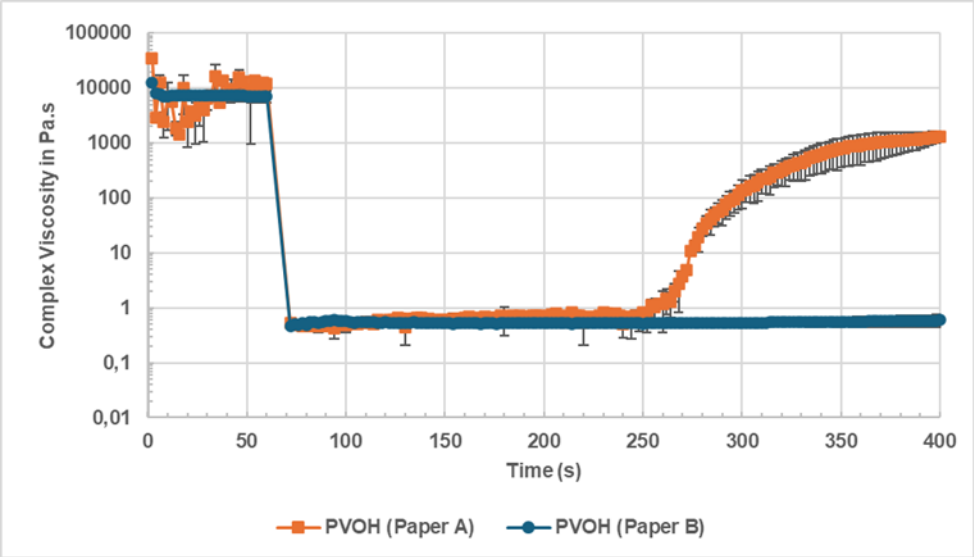

Figure 17. Complex viscosity during IMC measurements of PVOH coating on paper A (orange squares) and paper B (blue circles). The complex viscosity is shown as an average curve based on three replicates, with error bars indicating variability between measurements.

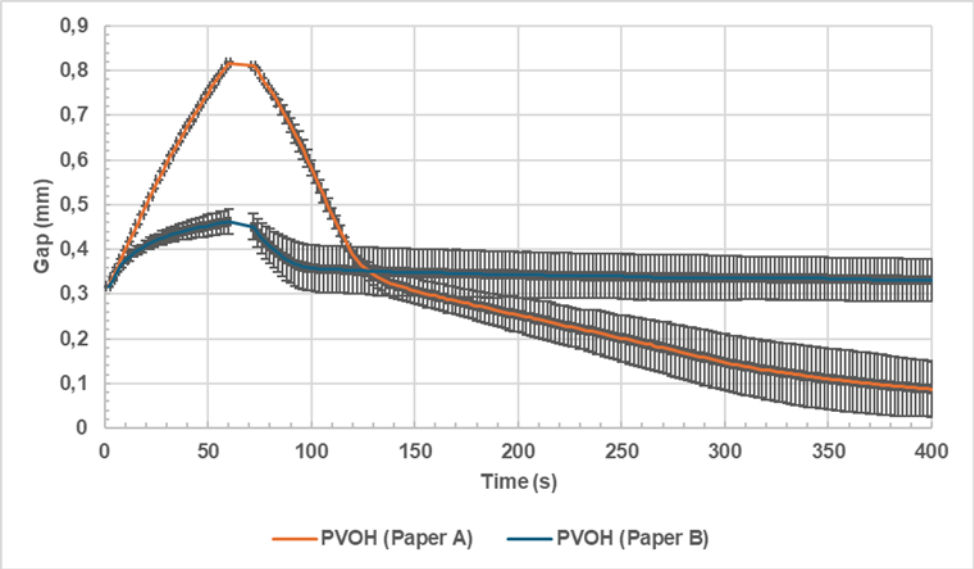

Figure 18. Gap during IMC measurements of PVOH coating on paper A (orange line) and paper B (blue line). The gap is shown as an average curve based on three replicates, with error bars indicating variability between measurements.

On paper A, the system shows a delayed but well-defined immobilization response. The viscosity remains low during the initial phase and begins to increase at approximately 250–270 s, reaching values of ~10^2–10^3 Pa·s. This transition is accompanied by continuous reduction in gap flow, decreasing from ~0.8 mm to below 0.1 mm, indicating progressive deposition of the coating layer.

In contrast, on paper B, no clear immobilization is observed within the measured time window. The viscosity remains nearly constant at low values (~0.5–1 Pa·s) and shows no significant increase throughout the experiment. Correspondingly, the gap shows only a limited decrease and stabilized at approximately ~0.33–0.35 mm, indicating minimal structural consolidation.

This behavior demonstrates that substrate properties strongly influence the onset and development of immobilization. While paper A supports sufficient dewatering to allow a delayed but observational transition, the restricted permeability of paper B limits liquid removal, preventing the system from reaching the conditions necessary for immobilization within the experimental timeframe.

4.1.2.3 Starch on Paper A and Paper B

For starch, substrate properties primarily affect the rate and sharpness of immobilization rather than its occurrence, as shown in Figure 19 and Figure 20.

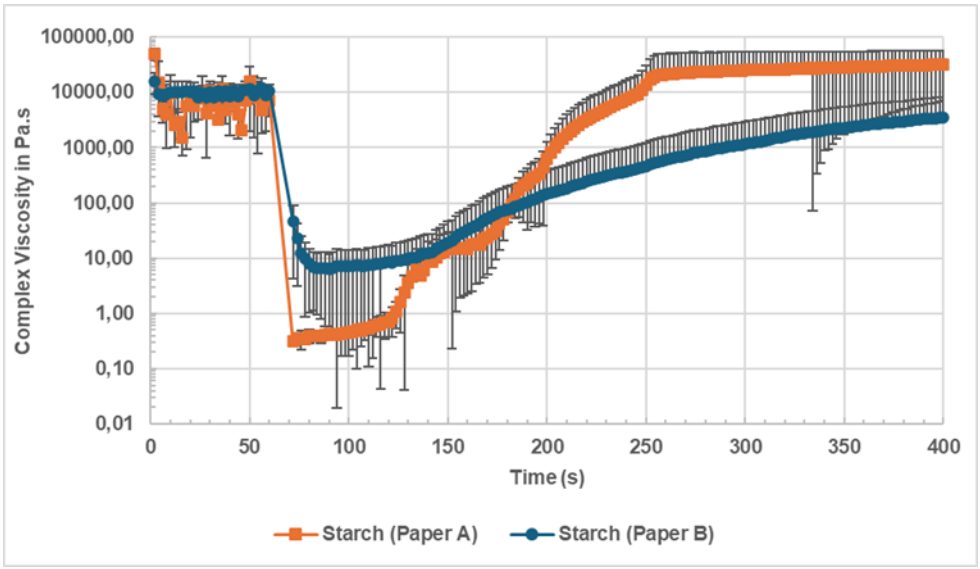

Figure 19. Complex viscosity during IMC measurements of starch coating on paper A (orange squares) and paper B (blue circles). The complex viscosity is shown as an average curve based on three replicates, with error bars indicating variability between measurements.

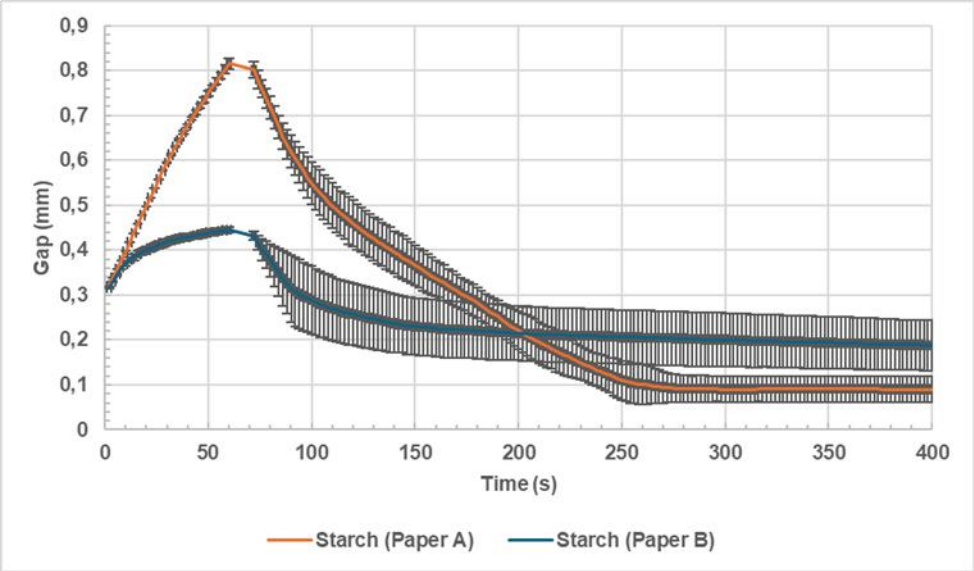

Figure 20. Gap during IMC measurements of starch coating on paper A (orange line) and paper B (blue line). The gap is shown as an average curve based on three replicates, with error bars indicating variability between measurements.

On paper A, immobilization occurs relatively early after pump activation, with a rapid increase in viscosity to high values (10^3–10^4 Pa·s) over a short interval. This transition is accompanied by a sharp decrease in gap, reaching values below ~0.1 mm, indicating rapid consolidation of the coating layer.

On paper B, the same system shows a delayed and more gradual transition. Viscosity increases more slowly over an extended time range, reaching comparable final values but with a less abrupt transition. The gap decreases continuously and stabilizes at higher values ~0.18–0.20 mm, suggesting that film formation proceeds over a longer time scale.

These differences can be attributed to the faster dewatering on paper A, which accelerates concentration build-up and an earlier transition. In contrast, the restricted permeability of paper B slows liquid removal, resulting in a more gradual evolution of viscosity and gap.

Importantly, immobilization occurs on both substrates, indicating that for starch systems, the substrate primarily influences the kinetics of the system to immobilize.

4.1.2.4 Silk Protein (60 mg/ml) on Paper A and Paper B

The silk protein systems present an intermediate response between starch and PVOH, with substrate properties influencing the rate and extent of immobilization. Figure 21 and Figure 22 shows the comparison of silk protein on Paper A and Paper B.

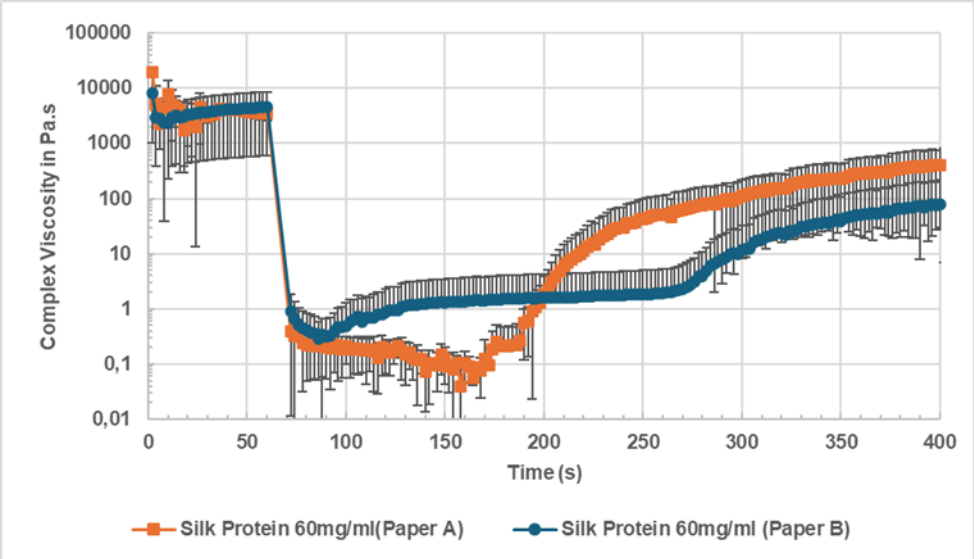

Figure 21. Complex viscosity during IMC measurements of silk protein (60mg/ml) coating on paper A (orange squares) and paper B (blue circles). The complex viscosity is shown as an average curve based on three replicates, with error bars indicating variability between measurements.

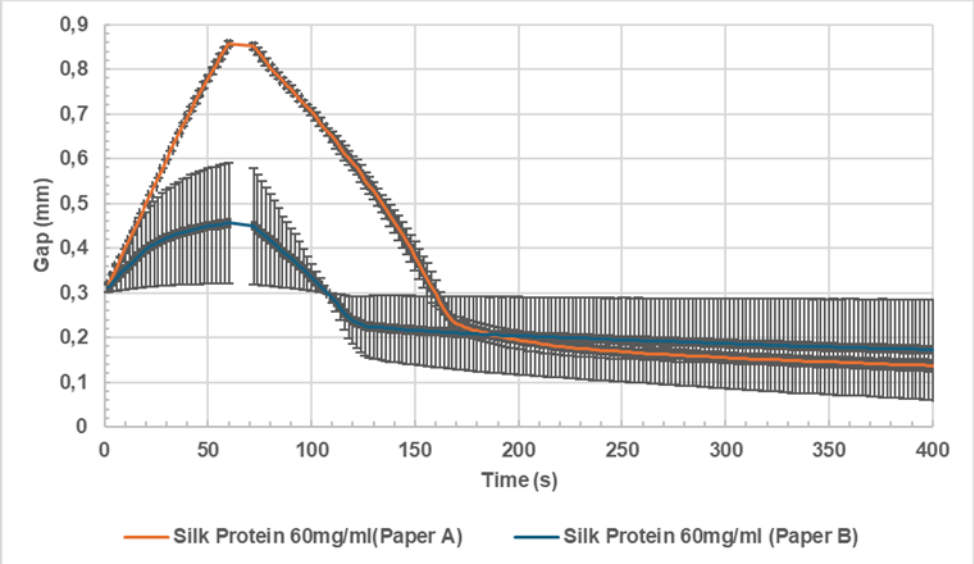

Figure 22. Gap during IMC measurements of silk protein (60mg/ml) coating on paper A (orange line) and paper B (blue line). The gap is shown as an average curve based on three replicates, with error bars indicating variability between measurements.

On paper A, viscosity increases progressively over time, beginning at approximately 190-210 s and reaching values on the order of ~10^2–10^3 Pa·s. This evolution is accompanied by a continuous reduction in gap, decreasing from 0.85 mm to approximately ~0.12 mm, indicating gradual film formation.

On paper B, both viscosity increases and gap reductions are slower and less pronounced. The onset of immobilization occurs later at ~260–280 s, and the final viscosity remains lower compared to paper A (~10^1–10^2 Pa·s). Similarly, the gap decreases more slowly and stabilizes at higher values (~0.15–0.18 mm), indicating delayed film formation.

In both cases, the evolution of viscosity and gap remains relatively smooth, without abrupt transitions. The primary effect of the substrate is therefore to delay and moderate the development of immobilization. In contrast to PVOH, where immobilization may be suppressed under limited dewatering conditions, the silk protein system continues to progress towards immobilization on both substrates, although at a reduced rate on paper B.

4.1.2.5 Substrate Influence Across Systems

Across all polymers, a consistent relationship is observed that substrate permeability governs the rate of dewatering, which in turn controls the development and kinetics of immobilization.

However, the extent of this influence varies depending on the polymer:

- PVOH shows a high sensitivity to substrate properties; immobilization occurs only under conditions of dewatering and is effectively suppressed on low-permeability substrates.
- In contrast, for Starch, the effect of the substrate is relatively limited, as immobilization occurs on both substrates. The primary difference lies in the rate of the transition.
- The silk protein system shows intermediate behavior. While immobilization is observed on both substrates, its progression is significantly slowed under restricted dewatering conditions.

These trends reflect how each paper responds differently to different polymers to substrate-controlled dewatering.

4.1.3 Role of Bulk Solution Properties in Immobilization Behavior

To further interpret the polymer-dependent immobilization behavior observed in section 4.1.1, additional characterization of the bulk solution properties was performed.

Rheological measurements and DLS analysis provide information about the stability of polymer systems. This is directly related to the previously discussed

immobilization mechanisms and therefore supports the interpretation of polymer-dependent behavior.

4.1.3.1 Rheological Behavior

Bulk rheological measurements were performed using cone-plate rheological instruments to characterize the viscoelastic behavior of the polymer solutions under closed-system conditions. The results are presented as frequency-dependent complex viscosity measurements conducted from day 0 to Day 1.

Figure 23 shows the complex viscosity of PVOH solutions (Day 0 - Day 3) as a function of frequency. The viscosity values lie in the range of approximately 0.6 to 1.2 Pa.s at low frequencies and decrease slightly with increasing frequency. The curves for all four days largely overlap across the entire frequency range, with only minor deviations observed at low frequencies, where day 1 shows slightly higher viscosity than the other days.

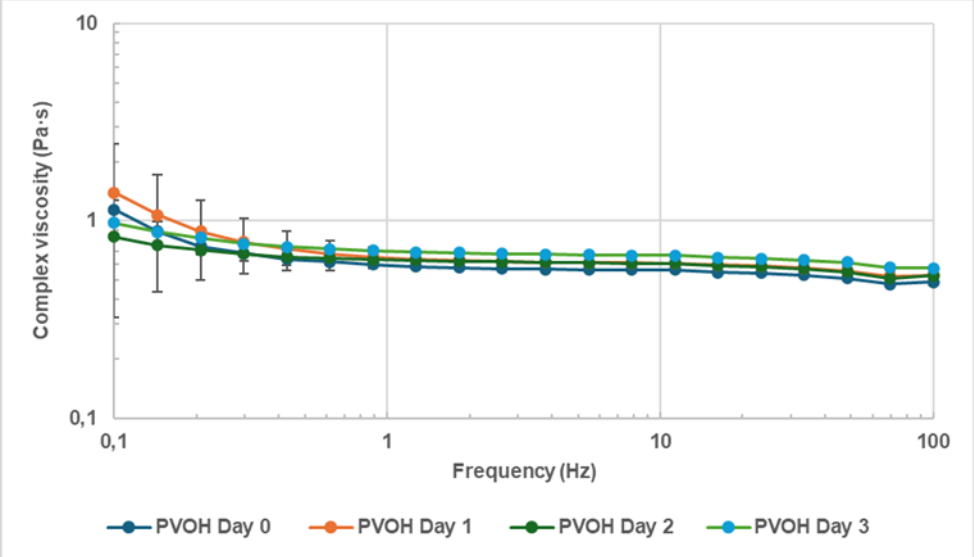

Figure 23. Frequency dependent complex viscosity of PVOH solutions measured over multiple days (Day 0–Day 3).

Figure 24 shows corresponding measurements for starch solutions. The viscosity values range from approximately 0.35 to 0.6 Pa·s. Compared to PVOH, a clearer separation between curves from different days is observed. Day 1 exhibits higher viscosity than day 0 across most of the frequency range. Day 2 shows a decrease in viscosity relative to day 1, while day 3 again shows a slight increase. The variation is consistent across the frequency range, and no strong frequency dependence is observed.

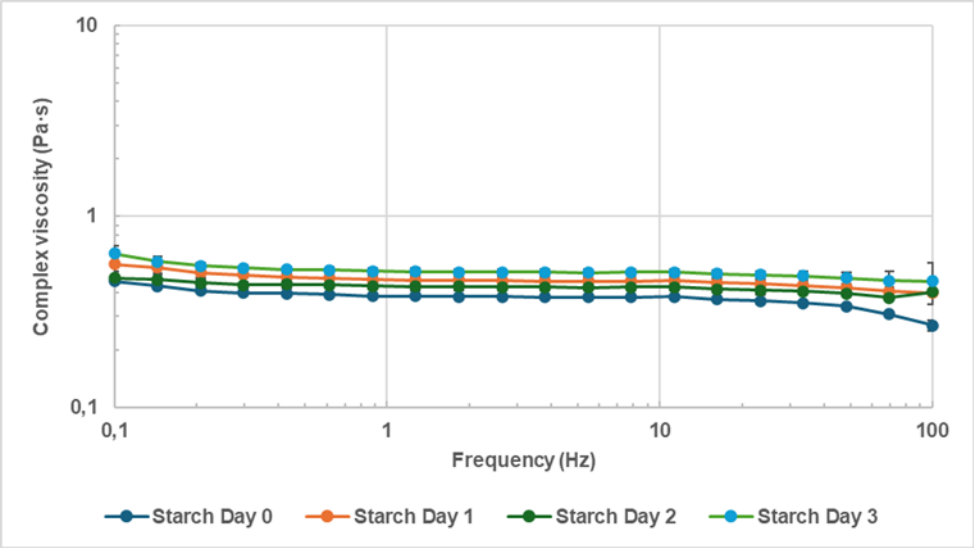

Figure 24. Frequency dependent complex viscosity of starch solutions over multiple days (Day 0–Day 3).

Figure 25 presents the rheological behavior of silk protein solution at a concentration of 40 mg/ml. The solution is shear thinning at low frequencies and shear thickening at high frequencies. A substantial difference between Day 0 and Day 1 is observed. The Day 0 curve lies in the range of approximately 0.05 and 0.8 Pa.s. In addition, to the increase in magnitude, the shape of the curve also differs between two days, with stronger frequency dependence observed in the Day 1 measurement.

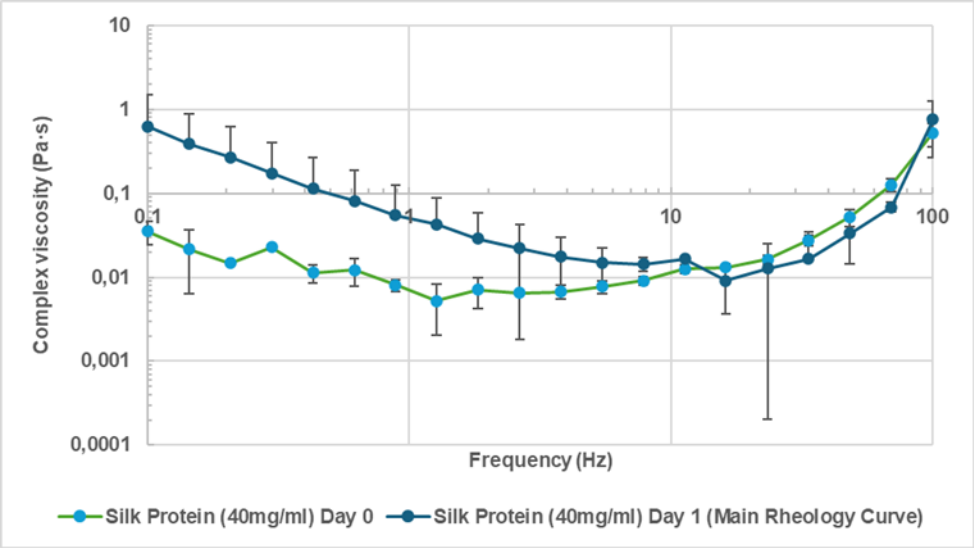

Figure 25. Frequency-dependent complex viscosity of silk protein solution (40 mg/mL) measured on Day 0 and Day 1.

For higher silk concentrations (60 and 76 mg/mL), complete multi-day rheological datasets were not available. Therefore, only limited qualitative observations were obtained for these systems.

4.1.3.2 Dynamic Light Scattering (DLS)

Dynamic light scattering (DLS) measurements were performed to characterize the dynamic behavior of the polymer solutions through the normalized intensity autocorrelation function $g^2(\tau) - 1$.

For clarity, only the back scattering results are presented here, as they show the most representative and least noisy behavior. Corresponding measurements obtained at 90° and forward scattering angles, which show consistent trends, are provided in Appendix B.

Figure 26 shows the correlation function of the PVOH solution measured over multiple days (Day 0-Day 3). The variation is consistent across the frequency range, and no strong frequency dependence is observed. At short delay times (approximately 0.1–10 μs), the Day 0 curve shows slightly higher initial correlation values compared to later measurements. As time increases, the separation between Day 0 and the other curves becomes more pronounced, with day 0 decreasing more rapidly. The curves for Day 1- Day 3 remain closely aligned over the entire time domain, indicating reproducible behavior across these measurements.

Similar trends are observed in the 90° and forward scattering configurations as shown in Figure B 1 and Figure B 2. Although the forward scattering measurements show lower overall signal intensity and increased noise, particularly at short times,

the distinction between Day 0 and subsequent days remains consistent across all scattering angles.

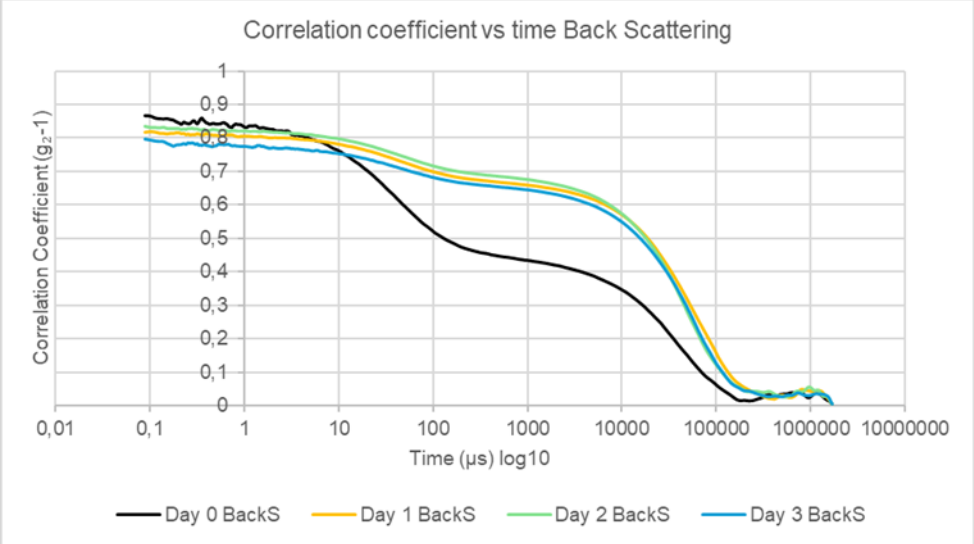

Figure 26. Normalized intensity autocorrelation function $g^2(\tau) - 1$ of PVOH solutions measured at back scattering over multiple days (Day 0 – Day 3).

Figure 27 shows the correlation functions of Starch solutions measured over multiple days (Day 0-Day 3).

Compared to PVOH, a clearer separation between curves for different days is observed. The Day 0 curve shows higher initial correlation values at short delay times (approximately 0.1–10 µs) and decays more gradually in the intermediate time range. In contrast, the curves for Day 1 and Day 3 largely overlap, indicating very similar decay behavior. The Day 2 curve shows slight deviations from this trend but remains close to the Day 1 and Day 3 measurements, particularly at intermediate and long delay times. At short delay times (approximately 0.1–10 µs), small variations between Day 1, Day 2, and Day 3 are visible. However, these differences are not systematic. At longer time scales, all curves gradually converge to similar values.

Similar trends are observed at 90° and forward scattering angles as shown in Appendix Figure B 3 and Figure B 4. Although forward scattering measurements show increased noise and lower overall correlation values, the relative relationship between the curves remains consistent, with Day 0 clearly separated from later measurements and Day 1 and Day 3 showing closely overlapping behavior.

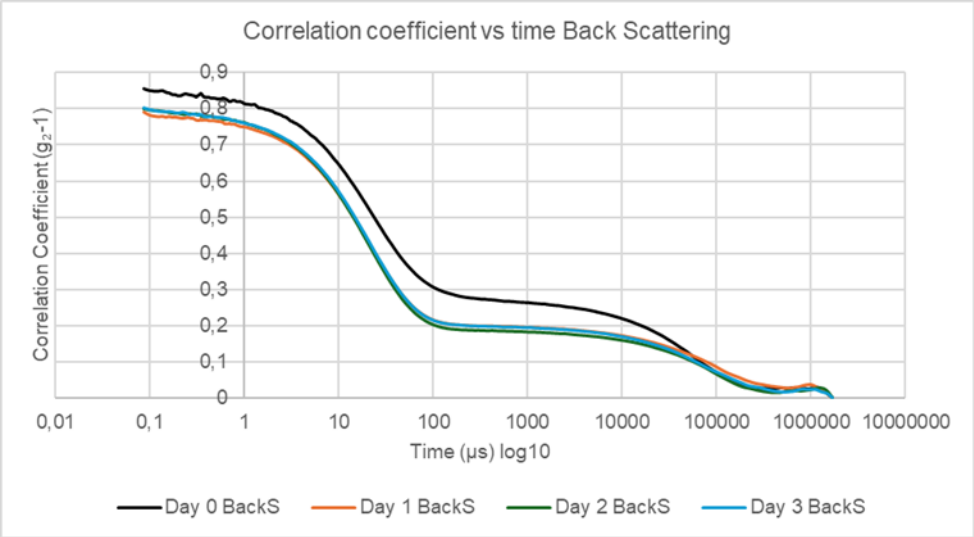

Figure 27. Normalized intensity autocorrelation function $g^2(\tau) - 1$ of starch solutions measured at back scattering over multiple days (Day 0-Day 3).

4.1.3.3 Correlation Between IMC, Rheological Behavior and DLS Measurements

Complementary characterization using bulk rheology and DLS was performed to evaluate the stability of the polymer solutions for the IMC measurements. Bulk rheological measurements using a cone-plate geometry demonstrated consistent viscosity behavior across different time points, with overlapping flow curves. Similarly, the DLS results showed no significant changes in particle size distribution over time, indicating that no structural degradation occurred during storage.

These observations confirm that the polymer solutions remained stable over the entire duration of the experiments. Therefore, variations observed in IMC measurements can be attributed to the dewatering process and concentration-driven structuring, rather than changes in the initial solution state. This validates the use of these solutions for IMC studies and ensures that the immobilization behavior reflects intrinsic material properties rather than time-dependent instability.

4.1.4 Influence of Experimental Conditions on IMC Behavior

In addition to intrinsic polymer properties and substrate effects, the IMC measurements are also influenced by experimental conditions associated with the measurement setup.

During the experiments, variations in IMC response were observed that could not be directly correlated with solution properties. Differences in signal stability and reproducibility were noted under varying operating conditions.

For example, measurements performed with immediate pump activation showed greater fluctuations in the recorded viscosity signal, particularly during the initial stages of the experiment. In contrast, introducing a short (60 s) stabilization period before suction resulted in smoother and more reproducible trends. Similarly, the application of non-zero normal force led to rapid, abrupt changes in the measured gap, accompanied by corresponding variations in the viscosity response. In addition, slight differences in suction efficiency of the pump across experiments resulted in variations in the rate of viscosity evolution during measurements. These variations were observed even under nominally identical experimental conditions. Representative examples illustrating the influence of experimental parameters on IMC measurements, including the effect of stabilization period and applied normal force, are provided in Appendix B.

These results demonstrate that experimental conditions represent an additional factor influencing IMC behavior, alongside polymer properties and substrate characteristics.

4.1.5 Coating Performance and Supporting Tests

4.1.5.1 Water Resistance Behavior (Cobb Test Results)

The water resistance behavior of coated papers and the uncoated reference paper on paper A was evaluated using the Cobb test. The measured Cobb45 values (30 s + 15 s) for all systems are summarized in Table 3.

The uncoated reference paper A shows the lowest water resistance, with an average Cobb45 value of approximately 3.1 g m^{-2}. This indicates a relatively high-water uptake compared to the coated samples. All applied coatings reduce water absorption. The PVOH-coated samples show an average Cobb45 value of approximately 2.4 g m^{-2}, indicating a decrease in water uptake compared to the reference. Similarly, silk protein coatings also reduce water absorption. The silk system at 40 mg mL^{-1} exhibits an average Cobb45 value of approximately 2.3 g m^{-2}, while the system at 76 mg mL^{-1} shows a slightly higher value of approximately 2.9 g m^{-2}. For the starch-coated samples, negative Cobb values were obtained indicating test failure, averaging approximately −0.5 g m^{-2}. The negative values can be due to mass loss, where the starch coating may have detached or dissolved during the test.

Table 3. Cobb45 values (30 s + 15 s) of uncoated and coated paper

System	Cobb45 value (g m^{-2})
Uncoated Reference paper A	3.1
Silk Protein (76 mg/ml) coating	2.9
PVOH coating	2.4

Silk Protein (40 mg/ml) coating	2.3
Starch coating	-0.5

A trend in water resistance is observed, where the uncoated reference paper exhibits the highest water uptake, followed by lower water uptake for silk and PVOH coatings, while starch showed signs of mass loss.

Reference Paper > Silk protein (76 mg mL^{-1}) > PVOH > Silk protein (40 mg mL^{-1})

4.1.5.2 Adhesion (Tack) Behavior of Coated Samples

The instant adhesion of the coated paper systems was evaluated using a qualitative tack test, where coating was applied between two papers, brought into contact and separated immediately (0 min) and after a short contact time (1 min). The extent of tack and fiber tearing was assessed visually, where fiber tear is associated with strong adhesion between the coating layer and the substrate.

Clear differences in adhesion behavior were observed between the investigated polymer systems on paper A.

For the PVOH system, no visible tack or fiber tear was observed at 0 min, indicating weak initial adhesion between the coated surfaces. After 1 min, fiber tear is observed, indicating adhesion, as the coated layers begin to interact more strongly. This reflects increasing interfacial bonding as water is redistributed within the coating layer.

In starch system, some fiber tearing is already observed at 0 min, indicating rapid adhesion development immediately upon contact with the coated surface. After 1 min, the extent of fiber tearing increases significantly, with large areas of coating transfer visible on both surfaces. This indicates strong interaction between the coating layers and the paper substrate. Furthermore, this behavior is consistent with the tendency of polysaccharide systems, such as starch, to rapidly form cohesive networks that promote rapid adhesion during drying.

For silk protein at 76 mg/ml, strong adhesion was observed already at 0 min, with significant fiber pull-out from the paper surface. This indicates that failure occurs within the substrate rather than at the interface between the two coated layers. This is typically associated with strong bonding between the coating and fiber network. Additional contact time does not result in noticeable changes, as adhesion is already high at initial contact. This is typically associated with strong bonding between the coating and fiber network.

For silk protein at 60 mg/ml, moderate adhesion behavior is observed. At 0 min, some fiber tearing is present, indicating partial interaction between the coated surfaces. After 1 min, the extent of fiber tearing increases, showing time-dependent adhesion development.

For silk protein at 40 mg/ml, no fiber tearing is observed at 0 min, indicating weak interaction between the coated surfaces. After 1 min, slight fiber tearing appears, suggesting gradual adhesion development over time.

Overall, the results show that adhesion develops differently across polymer systems and concentration. Systems such as starch and high-concentration silk protein (76 mg mL^{-1}) exhibit immediate adhesion upon contact, while PVOH and low-concentration silk showed delayed tack development. Fiber tearing observed in the tests indicates strong interaction between coating layers and the paper substrate, whereas clean separation suggests weak adhesion.

Table 4. Summary of adhesion (tack) behavior of different polymer systems at different contact times (0 = no effect/wet coating, + = moderate tack, some fiber tear, ++ = strong tack with fiber tear).

Polymer System	0 min contact	1 min Contact
PVOH	0	+
Starch	+	++
Silk Protein (76 mg/ml)	++	++
Silk Protein (60 mg/ml)	+	++
Silk Protein (40 mg/ml)	0	+

4.2 Discussion

4.2.1 Evaluation of the Main Hypothesis

The main hypothesis of this study proposes that the combined influence of intrinsic polymer properties, substrate-controlled dewatering, and experimental conditions governs immobilization behavior in water-based polymer coatings The results obtained in the work strongly support this statement, as none of these factors alone can fully explain the observed behavior.

The immobilization process in coating systems has been widely described as a coupled phenomenon involving dewatering and rheological evolution, where increasing solids concentration leads to rapid changes in mechanical response. The present findings are in direct agreement with this description, showing that structure formation becomes significant only after sufficient liquid removal has occurred. At the same time, the comparison between bulk measurements and IMC results demonstrates that immobilization cannot be understood solely in terms of intrinsic material properties. Literature consistently reports that coating behavior depends strongly on process-specific conditions such as shear, pressure and confinement, which influence the evolution of the structure during application. This is reflected in the differences observed between bulk and IMC behavior in this study (Willenbacher, Hanciogullari and Radle, 1999). Furthermore, substrate effects introduce an additional level of complexity. Liquid transport into porous substrate is governed by capillary forces and pore structure, which directly determines the rate of dewatering and, consequently, the onset of immobilization. This confirms that the process is strongly dependent on the interaction between coating and substrate (Mesic, Martinez-Hermosilla and Rättö, 2024).

Taken together, these findings clearly demonstrate that a single mechanism does not control immobilization behavior, but results from the interaction among polymer properties, substrate-controlled transport, and the experimental conditions. This provides strong support for the main hypothesis.

4.2.2 Polymer-Dependent Immobilization Behavior

The first supporting hypothesis (H1) states that polymers´ intrinsic properties exhibit distinct immobilization mechanisms due to differences in molecular structure and intermolecular interactions. The results strongly support this hypothesis and are consistent with established literature on polymer behavior.

As shown in the results, PVOH exhibits delayed, gradual immobilization process, indicating that structure formation occurs progressively rather than through a sharp transition to high viscosity. This behavior reflects fundamentally different

mechanisms, where molecular mobility remains sufficiently high to allow continued rearrangement during dewatering. PVOH is known to behave as an associating polymer, where hydrogen bonding of hydroxyl groups leads to the gradual formation of intermolecular connections as concentration increases. PVOH evolves toward a structured state through continuous chain association and entanglement (Parisi et al., 2022). From the perspective of fluid transport, the rate of solvent removal remains comparable to the rate of molecular rearrangement. As a result, the system does not reach a sudden percolation threshold. Instead, it undergoes progressive densification and structural evolution, as reflected in the smooth increase in viscosity and the gradual reduction in gap. This behavior is typical of film-forming polymers, where sufficient mobility enables surface leveling, pore-filling, and interfacial adaptation before final immobilization. In practice, PVOH behaves as a system that can reorganize during drying, resulting in more coherent and uniform film structures.

In contrast, starch exhibits the earliest and most abrupt immobilization behavior, indicating that structure formation occurs rapidly once a critical concentration is reached. This behavior is characteristic of percolation-controlled gelation, where the system transitions from a viscous liquid to a load-bearing network. From a molecular perspective, starch consists of amylose and amylopectin chains, both of which have a high density of hydroxyl groups, enabling extensive hydrogen bonding. Literature shows that starch systems can form three-dimensional hydrogen bonded networks, where polymer-polymer and polymer-water interactions lead to rapid gel formation once the overlap concentration is exceeded (Tako et al., 2014). The sharp increase in viscosity and abrupt gap collapse observed in IMC indicates that network formation occurs faster than solvent transport, leading to a mechanically rigid layer while dewatering is still ongoing. In this regime, further liquid removal does not induce flow but instead compresses an already-formed network. This behavior aligns with the literature, which describes starch as a strong film-forming and gelling agent, widely used in paper coatings to enhance bonding through dense network formation. However, such rapid immobilization also implies limited time for structural rearrangement, which can lead to non-uniform stress distribution and brittleness (Shen et al., 2012).

The silk protein system (particularly at 60 mg/ml) exhibits intermediate behavior, but its mechanism differs significantly from those of starch and PVOH. Immobilization is governed by aggregation-controlled dynamics, rather than classical gelation or progressive entanglement. Silk fibroin is known to undergo concentration-dependent self-assembly and aggregation, involving transitions from disordered structures to β-sheet rich configurations. These processes are highly sensitive to local concentration, shear, and dehydration conditions, leading to complex structural behavior (Trossmann, Lentz and Scheibel, 2023). In the present results, immobilization occurs on an intermediate timescale to starch and PVOH. This indicates that aggregation kinetics compete with solvent transport, leading to a system where structure formation is neither instantaneous nor fully continuous.

Importantly, the literature suggests that silk self-assembly at interfaces can involve localized aggregation, often leading to heterogeneity. However, the relatively smooth viscosity evolution observed here suggests that, under the applied IMC conditions, aggregation remains distributed and controlled rather than strongly localized. This is further supported by macroscopic observations of the coating, which appear continuous despite minor textural variations. This suggests that aggregation occurs throughout the film, contributing to structure development without leading to phase separation.

Bulk rheology and DLS provide useful information about initial solution state and stability, but they do not fully predict immobilization behavior under process conditions. This observation is consistent with previous studies on coating processes, which show that immobilization depends strongly on dewatering kinetics and concentration gradients, rather than solely on bulk rheological properties

Thus, these differences demonstrate that intrinsic polymer properties control the onset of immobilization, kinetics of structural development, and mechanical response during dewatering. However, immobilization behavior is fundamentally determined by how each polymer balances interaction strength, mobility, and aggregation dynamics, strongly supporting hypothesis 1.

4.2.3 Influence of Substrate Properties on Immobilization

The results demonstrate that substrate properties significantly influence immobilization behavior by controlling dewatering rate, thereby supporting Hypothesis 2. Water transport in paper substrates is governed by capillary forces and pore structure, which determines the rate of liquid absorption. Faster dewatering leads to rapid concentration increases and earlier immobilization, whereas slower dewatering delays this process (Mesic, Martinez-Hermosilla and Rättö, 2024).

From a mechanistic perspective, the substrate determines whether the system operates in a transport-limited regime, where solvent removal dominates, or a kinetically balanced regime, where molecular rearrangement and concentration increase occur simultaneously. As a result, systems with rapid structure formation (e.g., starch) immobilize regardless of substrate, whereas systems with slower structure development (e.g., PVOH) become highly sensitive to dewatering conditions.

Importantly, the substrate does not alter the underlying polymer interaction mechanism, but shifts the timing and evolution of immobilization, consistent with literature showing that dewatering controls immobilization kinetics rather than structure type (Willenbacher, Hanciogullari and Radle, 1999).

4.2.4 Role of Experimental Conditions and Process Effects

The results demonstrate that immobilization behavior is influenced not only by material properties and dewatering, but also by the experimental conditions under which the system is probed, confirming Hypothesis 3.

In IMC measurements, the coating is confined within a thin gap and subjected to oscillatory shear and normal forces while dewatering occurs. This creates a coupled mechanical environment in which the evolving structure is continuously deformed during concentration increase. As a result, immobilization reflects not only the formation of structure, but also the system´s ability to resist deformation under applied stress.

The reduction in the gap during measurement directly reflects that the volume above the paper is decreasing. However, this film formation is not purely a consequence of liquid loss but also depends on the mechanical strength of the developing structure. Systems that form rigid networks rapidly, such as starch, resist deformation and exhibit abrupt gap collapse, while more mobile systems, such as PVOH, show gradual densification due to ongoing structural rearrangement.

In addition, the applied normal force and oscillatory shear influence the distribution of stress within the coating layer. Under these conditions, structure formation occurs under load, meaning that immobilization represents a balance between internal network strength and externally applied mechanical forces. Similar effects have been discussed in the coating literature, where shear and pressure conditions influence the final coating structure (Willenbacher, Hanciogullari and Radle, 1999).

4.2.5 Functional Implication of Immobilization Behavior

The additional performance tests, including adhesion (tack) and Cobb measurements, provide further insight into the practical implications of the observed immobilization behavior.

The adhesion results reflect the strength and cohesion of the structures formed during immobilization. Systems exhibiting rapid structure formation, such as starch, show immediate fiber tearing, indicating the formation of a strong, rigid network. In contrast, systems with gradual immobilization behavior, such as PVOH, show delayed adhesion development, consistent with progressive intermolecular association and slower structure formation. For silk protein systems, adhesion behavior shows strong dependence on concentration. Higher concentrations lead to stronger and more immediate adhesion, which may correspond to increased intermolecular interactions and development of aggregated load-bearing structures.

Cobb measurements provide complementary information on water transport and absorption behavior. The results reflect how the formed coating structures influence liquid penetration and barrier properties. Systems that immobilize rapidly tend to

form denser structures at earlier stages, which can limit liquid transport, while systems with delayed immobilization allow continued penetration before structure formation is complete.

Overall, immobilization behavior arises from the combined effects of polymer interaction mechanisms, substrate-controlled dewatering, and process-dependent measurement conditions. The distinct pathways observed reflect how structure formation, transport, and mechanical constraints interact under dynamic conditions. These findings confirm that immobilization is a process-dependent phenomenon that link material properties to practical coating performance.

4.2.6 Implications for Sustainable Coating Systems

From a system level perspective, these findings directly address a central challenge in the transitions toward sustainable, paper-based packaging systems. As introduced earlier, replacing fossil-based barrier materials with renewable paper substrates requires not only material substitution but also precise control over coating functionality. Since paper is inherently porous and hydrophilic, achieving effective coating performance depends critically on the ability of the coating to form a continuous, defect-free film during dewatering.

The present work shows that this film formation process is fundamentally governed by immobilization, which emerges from a dynamic coupling between polymer interaction mechanisms, substrate-controlled dewatering kinetics, and process-induced mechanical conditions. This indicates that coating performance cannot be optimized solely through material selection but requires simultaneous control over transport phenomena and structure evolution during application. In particular, the results demonstrate that deviations in immobilization timing either earlier (as in starch) or delayed (as in PVOH) can lead to sub-optimal coating outcomes such as uneven film formation, excessive penetration, or reduced coating performance.

From a sustainability perspective, this highlights that the ability to tailor immobilization behavior of renewable materials through formulation and process parameters provides a pathway to optimize coating performance of environmentally favorable systems. In this context, the immediate behavior observed in silk protein illustrates the potential for designing materials that effectively balance flowability, structure formation, and functional performance.

Overall, this work demonstrates that controlling immobilization behavior is a key enabling factor in bridging the gap between sustainable material selection and high-performance coating applications in paper-based packaging.

4.2.7 Limitations of the Study

While the present study provides valuable insights into immobilization behavior, several limitations should be acknowledged.

One key limitation is the restricted range of polymer concentrations investigated. For PVOH and starch, only a single, industrially relevant concentration was ultimately used. Although preliminary experiments explored different concentrations, challenges related to stability and reproducibility of IMC measurements required the focus to shift toward establishing reliable experimental conditions. As a result, the systematic investigation of concentration on immobilization behavior was not in scope. For silk protein, small sample volumes of multiple concentrations (40,60, and 76 mg/ml) were considered; however, due to the limited sample availability, certain analysis were prioritized. Since silk protein represents a relatively new material in this application context, the study primarily focused on its behavior in IMC measurements.

The study was also limited to two paper substrates provided under confidentiality. Although quantitative data of substrate properties such as porosity and permeability were available, these numbers could not be disclosed. As a result, comparisons were restricted to qualitative descriptions, which limits the ability to generalize the findings to a broader range of substrates and reduces the level of quantitative interpretation.

Further limitations are associated with the performance tests. The tack measurements were qualitative and used primarily as a rapid indicator of adhesion behavior, without providing quantitative metrics. Cobb measurements showed uncertainties, particularly for starch systems, where structural effects and material loss during testing resulted in anomalous values. While this issue was not observed for all systems, it introduces some uncertainty in the quantitative interpretation of water resistance behavior.

From an experimental perspective, IMC measurements were found to be highly sensitive to operating conditions, including gap setting, procedure, onset of pump suction, and sample handling. This sensitivity led to measurement artefacts and variability, requiring careful evaluation and, in some cases, exclusion of outliers. In addition, practical challenges such as polymer precipitation and clogging within the system affected flow stability and required manual cleaning, introducing further variability in the measurements.

Overall, these limitations highlight the challenges related to experimental reproducibility, parameter control, sample handling, and data transparency, and they emphasize the need for further systematic and quantitative investigations to strengthen the immobilization measurements.

5 Conclusion and Recommendations

This chapter presents a comprehensive overview of the research's conclusions and recommendations for future research.

5.1 Conclusion

This work fundamentally reframes immobilization in water-based coating systems from a material property into a process-governed phenomenon. Rather than being defined by a fixed transition point, immobilization emerges as a dynamic outcome of competing mechanisms operating across multiple scales. At the molecular level, polymer-specific interactions determine how structure is organized, while at the macroscopic level, substrate-controlled aqueous transport regulates the rate at which this structure is developed. This interplay is further shaped by the mechanical constraints imposed by gap distance and normal force demonstrating that immobilization behavior arises from the coupled interaction of several factors.

The observed differences between PVOH, starch, and silk protein represent distinct mechanistic pathways governed by interaction strength, mobility, and aggregation behavior, thereby confirming the role of intrinsic polymer properties in defining how structure develops.

At the same time, substrate-controlled dewatering kinetics determine when this transition occurs. Faster aqueous transport accelerates concentration buildup and induces earlier immobilization, whereas slower transport delays or suppresses structure development. In addition, the influence of experimental parameters demonstrates that immobilization is inherently process-dependent, as confinement, oscillatory deformation, and measurement conditions define how the evolving layer responds under load.

Controlling immobilization is equivalent to controlling the competition between aqueous transport and rheological evolution. Systems that solidify too rapidly become transport-limited, leading to early locking and restricted film development, while systems that evolve too slowly remain dominated by fluid transport, resulting

in delayed structure formation and reduced adhesive performance. Optimal coating behavior therefore lies within a narrow regime where these processes are balanced.

The key contribution of the work is the demonstration that such balance can only be identified and quantified through process relevant measurements. By capturing the coupled evolution of viscosity and gap under relevant conditions, IMC can provide access to the dynamic pathways of immobilization that are not accessible through conventional bulk characterization methods. This establishes IMC as a useful tool for understanding and controlling immobilization in coating systems for emerging coating technologies.

5.2 Recommendations

Several aspects identified during this study suggest directions for future work. A key priority is to improve the consistency and reliability of IMC measurements by carefully studying important parameters such as gap setting, suction conditions, and oscillation inputs. Developing simple modelling approaches would also help to define suitable conditions and improve repeatability.

The effect of waiting time prior to measurement should be further explored, as different polymers and substrates may exhibit distinct stabilization and absorption behavior. Understanding this influence is important for ensuring consistent and comparable IMC measurements.

Error bars in complex viscosity proved useful for identifying data variability and should be explored further as a tool to assess measurement reliability.

Furthermore, additional data analysis approaches should be considered, such as evaluating the derivatives of the gap curves. Analysis of gap rate may provide deeper insight into the onset and progression of immobilization, as well as the identification of transition points such as knee regions, which are not fully captured by the gap profile alone.

A wider range of polymer concentrations should be investigated to better understand how concentration influences layer formation and immobilization behavior.

Improvements in the IMC setup are also needed, particularly to address issues such as pipe clogging and cleaning difficulties. A more stable and easy-to-maintain tube system would improve measurement reliability.

The silk protein solutions showed promising and reproducible behavior, and further work should explore silk´ potential properties for coating applications, including the use of scalable or bioengineered alternatives.

6 References

Alamri, M.S., Qasem, A.A.A., Mohamed, A.A., Hussain, S., Ibraheem, M.A., Shamlan, G., Alqah, H.A. and Qasha, A.S. (2021). Food Packaging materials: a Food Safety Perspective. Saudi Journal of Biological Sciences, 28(8), pp.4490–4499. doi:https://doi.org/10.1016/j.sjbs.2021.04.047.

Anton Paar. (n.d.). Basics of rheology | Anton Paar Wiki. [online] Available at: https://wiki.anton-paar.com/cn-cn/basics-of-rheology/.

Anton Paar (n.d.). Immobilization cell. Available at: https://www.anton-paar.com/corp-en/products/details/immobilization-cell/ (Accessed: 11 March 2026).

Arruda, T.R., Gabriela, Marques, C.S., Lelis, A., Maria, P.F., Oliveira, and Rafael, S. (2025). An Overview of Starch-Based Materials for Sustainable Food Packaging: Recent Advances, Limitations, and Perspectives. Macromol, [online] 5(2), p.19. doi:https://doi.org/10.3390/macromol5020019.

Bakker, S., Aarts, J., Esteves, C.C., Metselaar, G.A. and Albert (2022). Water Barrier Properties of Resin-Stabilized Waterborne Coatings for Paperboard. Macromolecular Materials and Engineering, 307(4). doi:https://doi.org/10.1002/mame.202100829.

Bauer, F., Nielsen, T.D., Nilsson, L.J., Palm, E., Ericsson, K., Fråne, A. and Cullen, J. (2022). Plastics and climate change—Breaking carbon lock-ins through three mitigation pathways. One Earth, [online] 5(4), pp.361–376. Available at: https://www.sciencedirect.com/science/article/pii/S2590332222001403.

Bing. (2025). HE EVALUATION OF THE PHYSICAL properties of a coated sheet concentrates primar - Bing. [online] Available at: https://www.bing.com/search?pglt=43&q=HE+EVALUATION+OF+THE+PHYSICAL+properties+of+a+coated+sheet+concentrates+primar&cvid=d021738fd3e24611b235170382738b89&gs_lcrp=EgRlZGdlKgYIABBFGDkyBggAEEUYOTIGCAEQRRg7MgYIAhBFGDsyCAgDEOkHGPxV0gEIMTA5MWowajeoAgCwAgA&FORM=ANNAB1&PC=U531

Boulet-Audet, M., Terry, A.E., Vollrath, F. and Holland, C. (2013a). Silk protein aggregation kinetics revealed by Rheo-IR. Acta Biomaterialia, [online] 10(2), pp.776–784. doi:https://doi.org/10.1016/j.actbio.2013.10.032.

Boulet-Audet, M., Terry, A.E., Vollrath, F. and Holland, C. (2013b). Silk protein aggregation kinetics revealed by Rheo-IR. Acta Biomaterialia, [online] 10(2), pp.776–784. doi:https://doi.org/10.1016/j.actbio.2013.10.032.

Christophliemk, H., Bohlin, E., Per Emilsson and Lars Järnström (2023a). Surface Analyses of Thin Multiple Layer Barrier Coatings of Poly(vinyl alcohol) for Paperboard. Coatings, 13(9), pp.1489–1489. doi:https://doi.org/10.3390/coatings13091489.

Eslami, H. and Mekonnen, T.H. (2023). Flexible and green multilayer paper coating for barrier enhancement of paper packaging. Sustainable Materials and Technologies, 37, p.e00694. doi:https://doi.org/10.1016/j.susmat.2023.e00694.

Gutoff, E.B. and Cohen, E.D. (2006). Coating and Drying Defects. doi:https://doi.org/10.1002/0470044136.

Horwood, A. and Nachiappan Chockalingam (2023). Principles of materials science. Elsevier eBooks, pp.91–174. doi:https://doi.org/10.1016/b978-0-323-85212-8.00002-x.

Human, G. (2025). Benefits of barrier coating for packaging. [online] Humanchem.com. Available at: https://global.humanchem.com/resources/benefits-of-barrier-coating-for-packaging.html [Accessed 25 May 2026].

Jader (2003). The immobilization cell revisited: Prediction of dewatering kinetics and immobilised layer properties for coating colours. Nordic Pulp & Paper Research Journal, [online] 18(04), pp.382–387. doi:https://doi.org/10.3183/NPPRJ-2003-18-04-p382-387.

Jain, A.C. and Cairncross, R.A. (n.d.). Moisture transport in paper and paper coatings. doi:https://doi.org/10.17918/etd-354.

Katashima, T. (2021). Rheological studies on polymer networks with static and dynamic crosslinks. Polymer Journal, [online] 53(10), pp.1073–1082. doi:https://doi.org/10.1038/s41428-021-00505-y.

Li, H., Qi, Y., Zhao, Y., Chi, J. and Cheng, S. (2019a). Starch and its derivatives for paper coatings: A review. Progress in Organic Coatings, 135, pp.213–227. doi:https://doi.org/10.1016/j.porgcoat.2019.05.015.

Luo, Y., Lee, Y.-F., Dennis, K.A., Velez, C., Brown, S.C., Furst, E.M. and Wagner, N.J. (2020). One-step, in situ jamming point measurements by immobilization cell rheometry. Rheologica Acta, [online] 59(4), pp.209–225. doi:https://doi.org/10.1007/s00397-020-01187-8.

Malik, M.I., Mays, J. and Shah, M.R. (2021). Molecular Characterization of Polymers. Elsevier.

Mesic, B., Martinez-Hermosilla, G.A. and Rättö, P. (2024). Effect of pressure and time on water absorption of coated paperboard based on a modified Cobb test method. TAPPI Journal, 23(4), pp.221–230.

Nature.com. (2025). Topic explorer | Nature Index. [online] Available at: https://www.nature.com/research-intelligence/nri-topic-summaries/silk-fibroin-and-its-biomedical-applications-micro-19345 [Accessed 25 May 2026].

NETZSCH - Analyzing and Testing. Leading in Thermal Analysis, Rheology and Fire Testing. (2025). Starch Pasting: Uncover RVA Curve Insights via Rheology. [online] Available at: https://analyzing-testing.netzsch.com/en-US/application-literature/starch-pasting-rva-curve-by-means-of-rheology.

Parisi, D., Ditillo, C.D., Han, A., Lindberg, S., Hamersky, M.W. and Colby, R.H. (2022). Rheological investigation on the associative properties of poly(vinyl alcohol) solutions. Journal of Rheology, [online] 66(6), pp.1141–1150. doi:https://doi.org/10.1122/8.0000435.

Pizzo, B., Chiozza, F. and Bernardini, F. (2024). Thermomechanical properties of poly(vinyl alcohol) prepared at room temperature as a function of degree of hydrolysis and aluminium addition. Polymer Degradation and Stability, 227, p.110887. doi:https://doi.org/10.1016/j.polymdegradstab.2024.110887.

Procopio, L. (n.d.). PAINT.ORG | TO CONTROL THE Rheology of paints and coatings. [online] Available at: https://www.paint.org/wp-content/uploads/2022/02/Additives-Rheology-of-Paints-and-Coatings_Oct-2021.pdf.

Procopio, L. (n.d.). PAINT.ORG | TO CONTROL THE Rheology of paints and coatings. [online] Available at: https://www.paint.org/wp-content/uploads/2022/02/Additives-Rheology-of-Paints-and-Coatings_Oct-2021.pdf.

Rizwan Shoukat, Cappai, M., Luca Pilia and Pia, G. (2025). Rice Starch Chemistry, Functional Properties, and Industrial Applications: A Review. Polymers, [online] 17(1), pp.110–110. doi:https://doi.org/10.3390/polym17010110.

Rodrigues, R. (2025). Rheology Basics and Testing Rheological Properties. [online] Analysis & Separations from Technology Networks. Available at: https://www.technologynetworks.com/analysis/articles/rheology-basics-and-testing-rheological-properties-395278.

Rockwood, D.N., Preda, R.C., Yücel, T., Wang, X., Lovett, M.L. and Kaplan, D.L. (2011). Materials fabrication from Bombyx mori silk fibroin. Nature Protocols, [online] 6(10), pp.1612–1631. doi:https://doi.org/10.1038/nprot.2011.379.

Saeed Paidari, Abdoreza Mohammadi Nafchi, Shima Vahedi, Morvarid Beigi, Sawsan Ali Al-Hilifi, Nafiseh Zamindar, Hosna Sajadizadeh, Abbasi, S. and Nateghi, L. (2024). Recent advances in protein-based coatings for food packaging: a review. Journal of Food Measurement & Characterization. doi:https://doi.org/10.1007/s11694-024-02491-0.

Santhosh, R., Ahmed, J., Thakur, R. and Sarkar, P. (2024a). Starch-based edible packaging: rheological, thermal, mechanical, microstructural, and barrier properties – a review. Sustainable Food Technology, [online] 2(2), pp.307–330. doi:https://doi.org/10.1039/D3FB00211J.

Scott Bader. (2025). Film Formation in Polymer Coatings. [online] Available at: https://www.scottbader.com/knowledge-hub/functional-polymers/film-formation-in-polymer-coatings/.

Seung, D. (2020). Amylose in starch: towards an understanding of biosynthesis, structure and function. New Phytologist, 228(5). doi:https://doi.org/10.1111/nph.16858.

Sharma, P., Kumar Agrawal, P., Singh, V., Chauhan, S. and Bhaskar, J. (1236). Jitendra Bhaskar (2023) A Comprehensive Review on Properties of Polyvinyl Alcohol (PVA) Crosslinked with Carboxylic Acid. J. Mater. Environ. Sci, [online] 2023(10), pp.1236–1252. Available at: https://www.jmaterenvironsci.com/Document/vol14/vol14_N10/JMES-2023-14107-Sharma.pdf.

Shen, J., Zhou, X., Wu, W. and Ma, Y. (2012). IMPROVING PAPER STRENGTH BY GELATION OF NATIVE STARCH AND BORAX IN THE PRESENCE OF FIBERS. BioResources, [online] 7(4). doi:https://doi.org/10.15376/biores.7.4.5542-5551.

Tako, M., Tamaki, Y., Teruya, T. and Takeda, Y. (2014). The Principles of Starch Gelatinization and Retrogradation. Food and Nutrition Sciences, 05(03), pp.280–291. doi:https://doi.org/10.4236/fns.2014.53035.

Trossmann, V.T., Lentz, S. and Scheibel, T. (2023). Factors Influencing Properties of Spider Silk Coatings and Their Interactions within a Biological Environment. Journal of functional biomaterials, 14(8), pp.434–434. doi:https://doi.org/10.3390/jfb14080434.

Wang, H.-Y., Zhang, Y., Zhang, M. and Zhang, Y.-Q. (2024). Functional modification of silk fibroin from silkworms and its application to medical biomaterials: A review. International Journal of Biological Macromolecules, 259, p.129099. doi:https://doi.org/10.1016/j.ijbiomac.2023.129099.

Wang, Q., Shi, A. and Shah, F. (2019). Rheology instruments for food quality evaluation. Evaluation Technologies for Food Quality, pp.465–490. doi:https://doi.org/10.1016/b978-0-12-814217-2.00018-4.

Willenbacher, N., Hanciogullari, H. and Radle, M. (1999). New laboratory test to characterize immobilization and dewatering of paper coating colors. TAPPI Journal, 82(8), pp.167–174.

Xie, F. and Liang, H. (2011). Effect of Concentration on Structure and Properties of Concentrated Regenerated Silk Fibroin Solution. Advanced Materials Research, 311-313, pp.1653–1656. doi:https://doi.org/10.4028/www.scientific.net/amr.311-313.1653.

Yang, L., Liu, J. and Gu, L. (2013a). DETAILED INSIGHTS TO LIQUID ABSORPTION AND LIQUID– PAPER INTERACTION. Trans. of the XVth Fund. Res. Symp. Cambridge, [online] pp.585–598. doi:https://doi.org/10.15376/frc.2013.2.585.

Yang, L., Liu, J. and Gu, L. (2013b). Trans. of the XVth Fund. Res. Symp. Cambridge, [online] pp.585–598. doi:https://doi.org/10.15376/frc.2013.2.585.

Appendix A

Project Time Plan

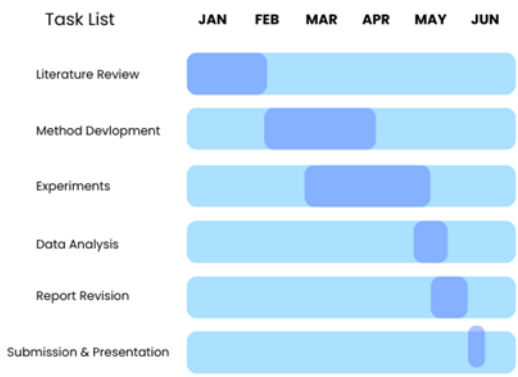

Ghent chart- Master´s Thesis Timeline (Jan-June 2026)

Appendix B

B.1 DLS Data: Side Scattering and Forward Scattering

B.1.1 PVOH

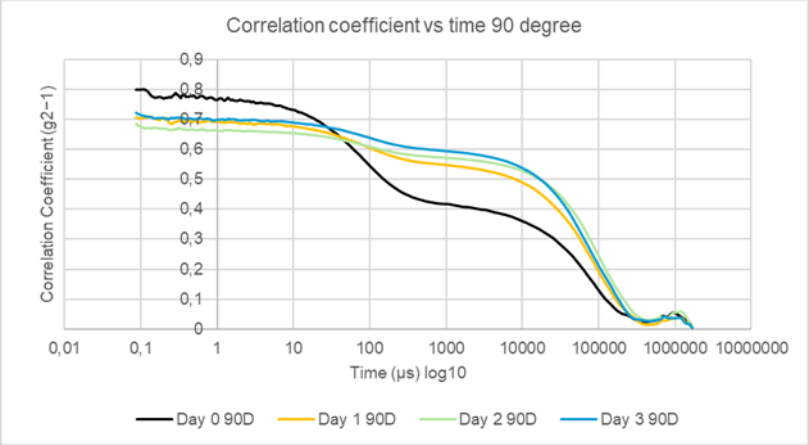

Figure B 1. Normalized intensity autocorrelation function $g^2(\tau) - 1$ of PVOH solutions measured at Side scattering over multiple days (Day 0 – Day 3).

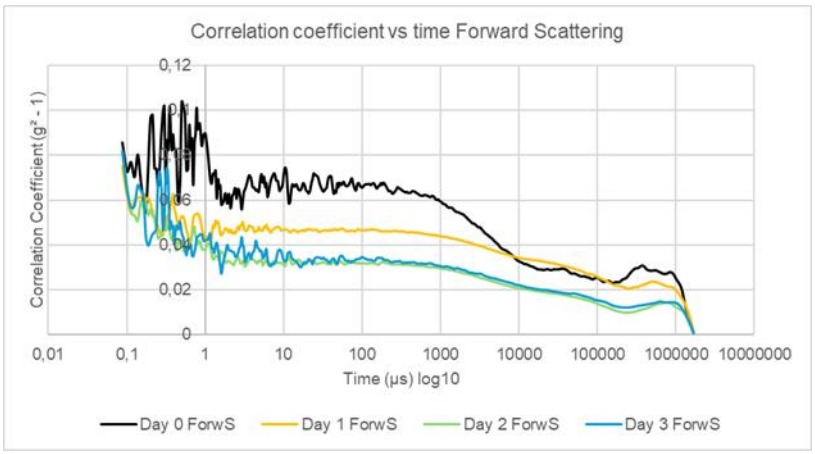

Figure B 2. Normalized intensity autocorrelation function $g^2(\tau) - 1$ of PVOH solutions measured at forward scattering over multiple days (Day 0 – Day 3).

B.1.2 Starch

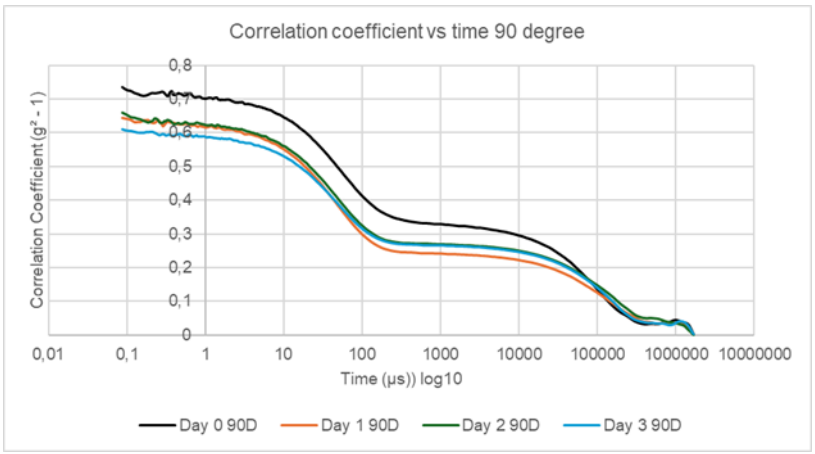

Figure B 3. Normalized intensity autocorrelation function $g^2(\tau) - 1$ of starch solutions measured at side scattering over multiple days (Day 0 – Day 3).

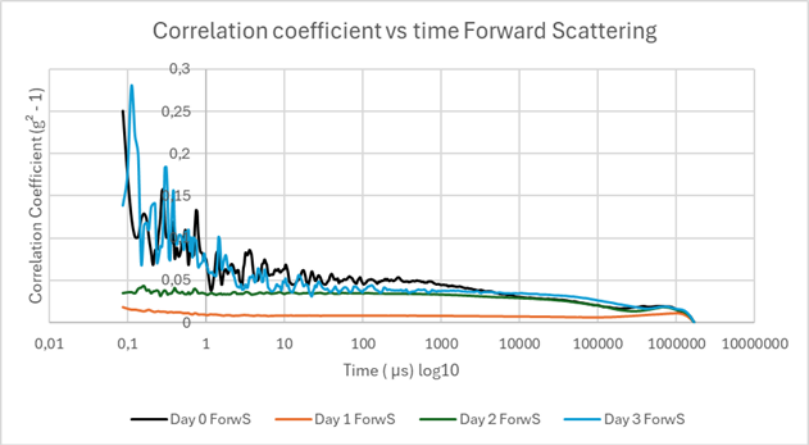

Figure B 4. Normalized intensity autocorrelation function $g^2(\tau) - 1$ of starch solutions measured at forward scattering over multiple days (Day 0 – Day 3).

B.2 Influence of Varying Experimental Parameters on the Final Failure Response

B.2.1 Influence of Applied Force (1N)

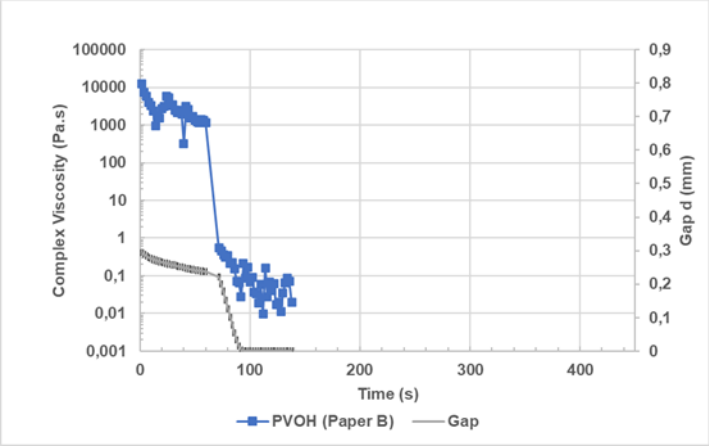

Figure B 5. Complex viscosity and gap evolution of PVOH (Paper B) under constant conditions (pump off for 60 s, 30 data points) with force increased from 0 to 1 N.

B.2.2 Effect of Immediate Pumping

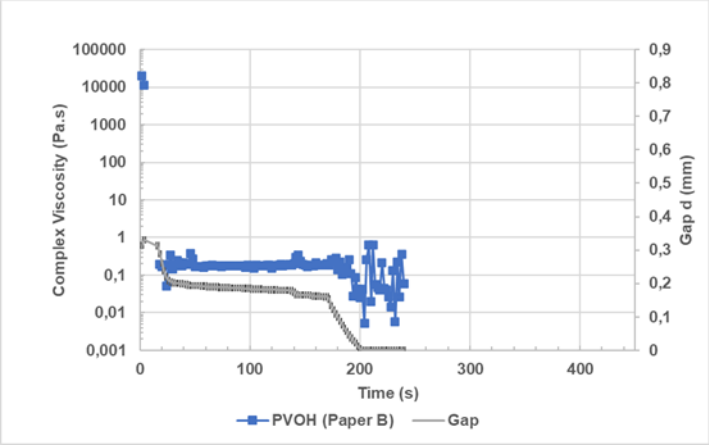

Figure B 6. complex viscosity and gap evolution of PVOH (Paper B) with no initial waiting time, where the pump is started immediately.

B.2.3 Effect of Gap Calibration

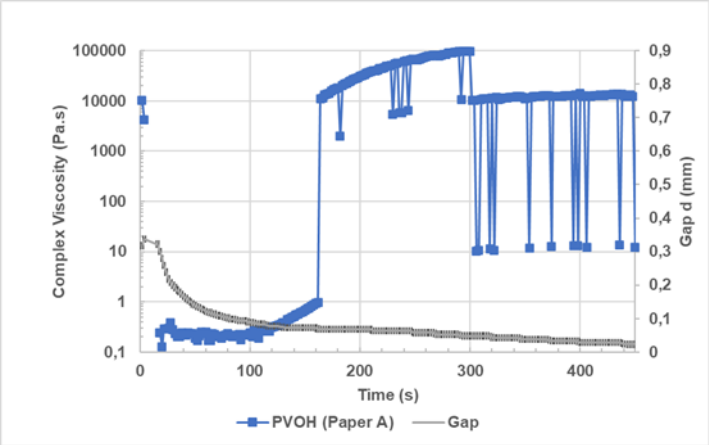

Figure B 7. complex viscosity and gap evolution of PVOH (Paper A) when the gap was zeroed on the paper substrate instead of the steel plate, showing irregular measurement behaviour.

Appendix C

C.1 Circular Paper-Based Coated Samples

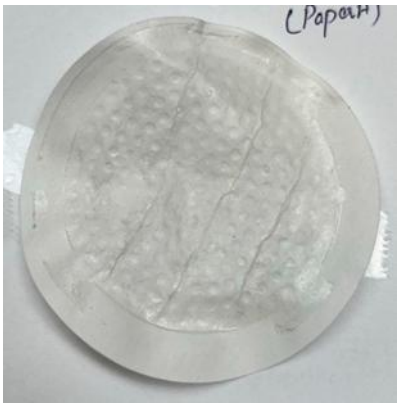

Figure C 1. Coated PVOH sample on paper A

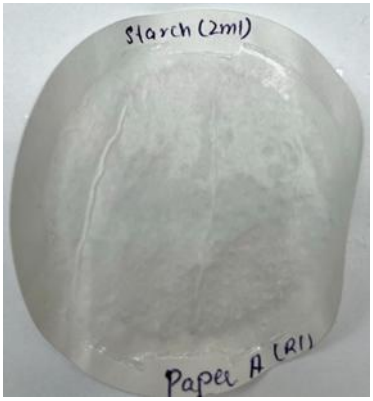

Figure C 2. Coated starch sample on paper A

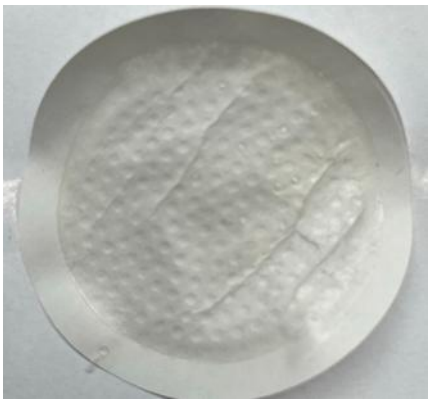

Figure C 3. Coated silk protein (60 mg/ml) sample on paper A.

C.2 Adhesion (Tack Test)

Figure C 4. Adhesive test of starch coated paper at 1 min